Rational Design of High Performance Conjugated Polymers for Organic Solar Cells — Source link ↗

Huaxing Zhou, Liqiang Yang, Wei You

Institutions: University of North Carolina at Chapel Hill

Related papers:

- Molecular design of photovoltaic materials for polymer solar cells: toward suitable electronic energy levels and broad absorption.

- Synthesis of Conjugated Polymers for Organic Solar Cell Applications

- Polymer photovoltaic cells : enhanced efficiencies via a network of internal donor-acceptor heterojunctions

- Design Rules for Donors in Bulk-Heterojunction Solar Cells—Towards 10 % Energy-Conversion Efficiency

- Enhanced power-conversion efficiency in polymer solar cells using an inverted device structure

Rational Design of High Performance Conjugated Polymers for Organic Solar Cells

Huaxing Zhou,[†] Liqiang Yang,[‡] and Wei You*,[†,‡]

[†]Department of Chemistry, University of North Carolina at Chapel Hill, Chapel Hill, North Carolina 27599-3290, United States

[‡]Curriculum in Applied Sciences and Engineering, University of North Carolina at Chapel Hill, Chapel Hill, North Carolina 27599-3287, United States

ABSTRACT: The research on the polymer-based solar cells (PSCs) has attracted an increasing amount of attention in recent years because PSCs pose potential advantages over mainstream inorganic-based solar cells, such as significantly reduced material/fabrication costs, flexible substrates, and light weight of finished solar cells. The research community has made great progress in the field of bulk heterojunction (BHJ) polymer solar cells since its inception in 1995. The power conversion efficiency (PCE), a key parameter to assess the performance of solar cells, has increased from 1% in the 1990s to over 8% just recently. These great advances are mainly fueled by the development of conjugated polymers used as the electron-donating materials in BHJ solar cells. In this Perspective, we first briefly review the progress on the design of conjugated polymers for polymer solar cells in the past 16 years. Since a conjugated polymer can be arbitrarily divided into three constituting components—the conjugated backbone, the side chains, and the substituents—we then focus on the rational design of conjugated polymers by separately discussing the influence of each component on the physical and photovoltaic (PV) properties of these polymers. Special attention is paid to the design of donor–acceptor type low-band-gap polymers because this approach is prevailing in the literature with its unique features. In doing so, we strive to extract useful rules for the rational design of conjugated polymers with predictable properties. We conclude by proposing future research opportunities to achieve even higher PCEs for PSCs.
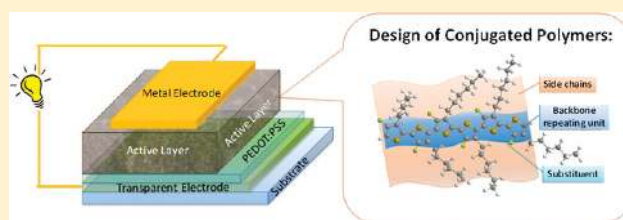
1. INTRODUCTION

1.1. Background. Polymer solar cells (PSC) have attracted an increasing amount of attention in the research community due to the potential advantages of PSC over inorganic-based solar cells, including low cost, light weight, and fast/cheap roll-to-roll production.[1–7] Typically, p-type semiconductor (i.e., electron DONOR, such as conjugated polymers) and n-type semiconductor (i.e., electron ACCEPTOR, such as fullerene derivatives) are blended in a bulk heterojunction (BHJ) configuration as the core component for PSC.[3] The interpenetrated network of BHJ offers two advantages: (a) it minimizes the traveling distance of excitons (electron−hole pair generated upon light absorption) to the DONOR/ACCEPTOR (D/A) interface and concurrently maximizes the D/A interfacial area, thereby ensuring the exciton dissociation at the D/A interface to generate maximum free charge carriers; (b) it offers charge transport pathways to facilitate the charge collection at electrodes, completing the conversion of the photon energy to electrical energy (i.e., photovoltaic effect). In a complete BHJ solar cell, the active layer is sandwiched between a transparent anode (typically tin-doped indium oxide, ITO) and a metal cathode (Figure 1). Additionally, a thin layer of poly(3,4-ethylenedioxythiophene)−poly(styrenesulfonate) (PEDOT:PSS) is generally applied in between the ITO and the active layer to improve the electrical contact between the ITO and the active layer and to adjust energy levels.[8]
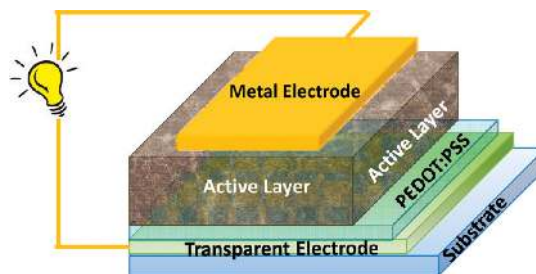
Figure 1. Schematic illustration of the structure of a typical bulk heterojunction polymer solar cell device.

The power conversion efficiency (PCE) of polymer solar cells has improved rapidly from below 1% to over 8% in the past 16 years.[9] This impressive accomplishment is mainly achieved by the molecular engineering of the structure of conjugated polymers (as the DONOR materials),[10–12] assisted by limited successes in derivatizing the fullerenes (as the electron ACCEPTOR).[12–18]

Because of the limited solubility of buckminsterfullerene (C_{60}) in common organic solvents, a fullerene derivative, [6,6]-phenyl-C61-butyric acid methyl ester ($PC_{61}BM$), has been used as

a standard and efficient ACCEPTOR material in PSC. The photoinduced charge transfer from the conjugated polymer to $PC_{61}BM$ occurs quantitatively on the picosecond time scale with exciton dissociation rate near unity,[3] a unique feature inherited from the original C60.[19] Although some other high performance fullerene derivatives have also been developed over the years,[12−18,20] the relatively cheap and commercially available $PC_{61}BM$ is still widely applied as the standard ACCEPTOR material. In recent years, $PC_{71}BM$, a C_{70} analogue of $PC_{61}BM$, was used in some research groups to increase PCE because of its better light absorption in the visible region.[15] *In this Perspective, we will focus on the rational design of conjugated polymers under the assumption that $PC_{61}BM/PC_{71}BM$ is used as the electron ACCEPTOR.* The seemingly narrow topic of conjugated polymer-based solar cells in fact covers a much wider range of active research thrusts, ranging from materials synthesis, physical chemistry (e.g., exciton behavior and morphological study of active layers), to device physics and involves multiple disciplines (chemistry, physics, and engineering). Therefore, interested readers should refer to other related reviews to grasp a more comprehensive picture of the extremely active and productive field of polymer solar cells.[10,12,21−33] Finally, to avoid confusion, donor and acceptor are generally referred to as building units for the design of polymers, while DONOR and ACCEPTOR with all letters capitalized are reserved to represent the DONOR polymer and ACCEPTOR (e.g., fullerene) in the BHJ blend, respectively.

1.2. A Brief History of the Development of Conjugated Polymers for Polymer Solar Cells. The rather short history of BHJ solar cells can be roughly divided into three phases from the perspective of the conjugated backbones of DONOR polymers. Phase one centered on poly(phenylene vinylene)s (PPV), such as poly[2-methoxy-5-(2′-ethylhexyloxy)-1,4-phenylenevinylene] (MEH-PPV) and poly[2-methoxy-5-(3′,7′-dimethyloctyloxy)-1,4-phenylenevinylene] (MDMO-PPV). Power conversion efficiency as high as 3.3% was achieved in PPV-based BHJ solar cells with $PC_{61}BM$ as the ACCEPTOR material, mainly through the application of chlorinated solvents to tune active layer morphologies.[34,35] A high open-circuit voltages (V_{oc}) up to 0.82 V was obtained as a result of the relatively low highest-occupied molecular orbital (HOMO) energy level of −5.4 eV of MDMO-PPV; however, the large band gap of MDMO-PPV limited the short-circuit current density (J_{sc}) to 5−6 mA/cm². Therefore, in phase two, a smaller-band-gap polymer, regioregular poly(3-hexylthiophene) (rr-P3HT), was thoroughly investigated.[27] P3HT-based BHJ devices provide a noticeably higher current density (over 10 mA/cm²), attributed to its lower band gap (1.9 eV) as well as to its increased π-stacking and crystallinity which yields a higher hole mobility.[36−38] Upon optimization of the active layer morphology via thermal[38] or solvent annealing,[39] an impressive PCE of 5% was achieved.[27,40] Unfortunately, the high HOMO (− 5.1 eV) energy level of P3HT has restricted the V_{oc} to ∼0.6 V in its related BHJ solar cells with $PC_{61}BM$ as the ACCEPTOR, which consequently limits the overall efficiency.

Presently in phase three, numerous polymer backbones have been reported. High V_{oc} over 1 V,[41−43] high J_{sc} over 17.3 mA/cm²,[5] and fill factor (FF) over 70%[44,45] have been demonstrated in different polymer-based BHJ solar cells. If all these impressive values could be combined in one polymer solar cell, it would give a PCE as high as 12%! However, due to the interplay of polymer properties such as energy levels and band gap and their correlation with V_{oc} and J_{sc}, highest V_{oc} and highest J_{sc} cannot be concurrently obtained.[46] In order to achieve the highest possible PCE, one needs to carefully balance

the V_{oc} and J_{sc} via judicious control over physical properties of a conjugated polymer (i.e., in pursuit of "ideal polymers").

1.3. Required Properties for Ideal Polymers. To design ideal polymers as the DONOR in polymer-based BHJ solar cells with high PCE (PCE = $V_{oc} \times J_{sc} \times FF/P_{in}$), the following issues need to be carefully addressed.

a. Open-Circuit Voltage (V_{oc}). V_{oc} is tightly correlated with the energy level difference between the HOMO of the DONOR polymer and the LUMO of the ACCEPTOR (e.g., $PC_{61}BM$).[47] In theory, polymers with low-lying HOMO levels would exhibit higher V_{oc}. However, the HOMO level of the DONOR polymer cannot go too low. This is because generally a minimum energy difference of ∼0.3 eV between the LUMO energy levels of the DONOR polymer and the ACCEPTOR is required to facilitate efficient exciton splitting and charge dissociation. When $PC_{61}BM$ with a LUMO level of −4.2 eV is used as the ACCEPTOR, the lowest possible LUMO level of the DONOR polymer would be near −3.9 eV. Continuously lowering the HOMO level of the DONOR polymer would inevitably enlarge the band gap of the polymer, diminishing the light absorbing ability of the DONOR polymer (thereby a low J_{sc}). The origin of V_{oc} is still under intense debate, and recent data indicate that V_{oc} is decided by a couple of other factors besides just the HOMO level of the polymer.[48,49] Furthermore, bulkiness of side chains, interchain distances, and morphology of active layer have also been demonstrated to have a noticeable effect on the V_{oc}.[50]

b. Short-Circuit Current (J_{sc}). The theoretical upper limit for J_{sc} of any excitonic solar cell is decided by the number of excitons created during solar illumination. Ideally, the absorption of the active layer should be compatible with the solar spectrum to maximize the exciton generation. Since $PC_{61}BM$ has a poor absorption in the visible and near-IR region where most of the solar flux is located, the DONOR polymer has to serve as the main light absorber. Roughly 70% of the sunlight energy is distributed in the wavelength region from 380 to 900 nm;[51] hence, an ideal polymer should have a broad and strong absorption in this range, which requires the polymer band gap to be 1.4−1.5 eV. A narrower band gap polymer could absorb more light, which would increase the J_{sc}; however, continuing to lower the band gap would require an increase of the HOMO level of the DONOR polymer (since the LUMO level cannot be lower than −3.9 eV with $PC_{61}BM$ as the ACCEPTOR for efficient exciton splitting and charge dissociation)[21] and would reduce the V_{oc}.

If one assumes a fill factor of 0.65, an external quantum efficiency of 65%, and an optimal morphology, one can approximate the overall PCE from the optical band gap and the LUMO/HOMO of the DONOR polymer in a polymer:$PC_{61}BM$ BHJ solar cell (Figure 2).[47] It is clearly seen that a PCE of 10% can be achieved by an "ideal" polymer with an optimal band gap of 1.5 eV and a HOMO level around −5.4 eV.

Though the experimentally determined V_{oc} can be very close to the predicted value based on the measured HOMO level of the polymer, the actual J_{sc} extracted from a polymer solar cell is usually significantly lower than the theoretical J_{sc} due to a number of loss mechanisms (e.g., monomolecular or bimolecular recombination) during the charge generation, transport, and extraction.[22,51] Thus a few other desirable features need to be included to mitigate these losses, such as high molecular weight, high charge mobility, and optimized active layer morphology, all of which will help improve the actual J_{sc}.

c. Fill factor (FF). From a semiconductor photovoltaic device point of view, a high FF requires a small series resistance (R_s) and a large shunt resistance (R_{sh}),[52] both of which are
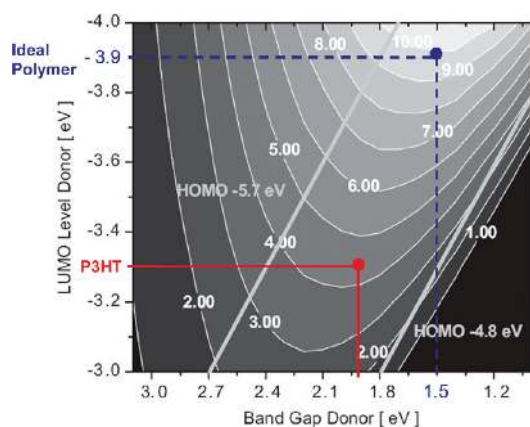
Figure 2. Calculated energy-conversion efficiency of P3HT and an "ideal" polymer, assuming *FF* and IPCE at 65%. Reprinted with permission from ref 47. Copyright 2006 Wiley-VCH Verlag GmbH & Co. KgaA.

significantly impacted by the morphology of the polymer/fullerene blend. Thus, the morphology of the active layer should be optimized to promote charge separation and favorable transport of photogenerated charges in order to maximize the *FF* and the attainable J_{sc}.

Finally, besides high PCE, solution processability (offered by side chains) and long-term stability of polymer solar cells (related with both materials and encapsulation) are of equal importance for future application and commercialization.

In short, the properties desired for a high performance polymer are (1) good solubility, (2) high molecular weight, (3) HOMO level around −5.4 eV, (4) LUMO level around −3.9 eV, (5) high hole mobility, (6) optimal morphology, and (7) long-term stability.

2. MOLECULAR ENGINEERING OF CONJUGATED POLYMERS FOR POLYMER SOLAR CELLS

2.1. Structural Features of Conjugated Polymers: A Bird's Eye View.
A typical conjugated polymer used as the electron DONOR in polymer solar cells is illustrated in Scheme 1.

Scheme 1. Illustration of a Typical Conjugated Polymer for Polymer Solar Cells
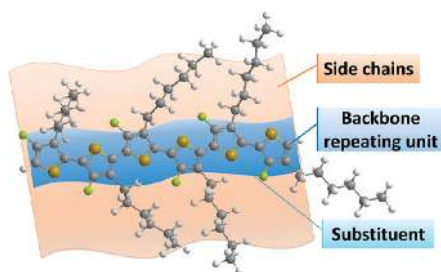
Generally, a conjugated polymer can be arbitrarily divided into three constituting components: the conjugated backbone, the side chains, and the substituents. The conjugated backbone is the most important component because it dictates most of the PSC-related physical properties of the conjugated polymer, such as energy levels, band gap, and inter/intra molecular interactions. Hundreds of different backbones have been reported so far;[10−12] however, the design of polymer backbones has been quite empirical. As a result, the discovery of high performance polymers is

rather serendipitous. Therefore, the rational design of conjugated backbone (i.e., the repeating units) is of utmost importance in the further development of polymer solar cells.

On the other hand, side chains play a crucial role in improving the molecular weight, solubility, and processability of conjugated polymers. Furthermore, these side chains can adjust intermolecular interactions and allow proper mixing with $PC_{61}BM$ to form the desired morphology. However, these insulating side chains also dilute the chromophore density and disturb π-stacking of polymer backbones, which could thwart the light absorption and charge transport. In addition, improper attachment of side chains may introduce steric hindrance and twist the conjugated backbone, which could lead to a large band gap, low charge carrier mobility, and poor photovoltaic properties. Finally, there are increasing evidence showing that the shape and length of side chains have noticeable impact on the photovoltaic properties of conjugated polymers.

Lastly, substituents (such as F and CN) are generally used as fine-tuning methods to tweak the physical properties of conjugated polymers, particularly the electronic properties (energy levels, band gap, mobility, etc.). Since photovoltaic properties of conjugated polymers are very sensitive toward their electronic properties, sometimes substituents can have important influence on the photovoltaic performance of related conjugated polymers.

2.2. Rational Design of Conjugated Polymer Backbones.
All reported conjugated backbones for PSC can be arbitrarily classified into a few categories based on the constitution of the repeating unit, namely (a) homopolymer, (b) donor−acceptor polymer, (c) quinoid polymer, and (d) other types of polymers, as shown in Figure 3.

The repeating unit of the homopolymer usually consists of a single aromatic unit or fused aromatics. The physical properties of these polymers are largely determined by the intrinsic properties of the constituting single or fused aromatics, with appreciable contribution from steric hindrance between these repeating units. Thus, most of the homopolymers have large band gaps (>1.9 eV), which limit the light absorption of these materials. In addition, very often the aforementioned steric hindrance forces the adjacent repeating units off the desired coplanarity of these units, negatively impacting the band gap and the crystallinity of the polymer, thereby diminishing photovoltaic properties of related BHJ devices.[40,53,54] The best polymer of this type is the regioregular P3HT with PCE over 5% after thorough optimizations.[27,38,40]

On the other hand, it is fairly easy to construct low-band-gap polymers with tunable energy levels via the donor−acceptor (D−A) approach. The repeating unit of D−A polymers comprises of an electron-rich "donor" moiety and an electron-deficient "acceptor" moiety. The internal charge transfer between the "donor" and the "acceptor" moieties leads to the observed low band gap.[55] This strategy was first proposed in 1993[56,57] and best illustrated by Tour et al. by using a copolymer of 3,4-aminothiophene and 3,4-nitrothiophene to reach a band gap of 1.0 eV, as shown in Figure 3.[58] The internal charge transfer (ICT) intrinsic with the D−A structure leads to more desirable double-bond characteristic between repeating units. Therefore, the conjugated backbone adopts a more planar configuration to facilitate the π-electrons delocalization along the conjugated backbone, leading to a smaller band gap. One unique feature of the D−A polymers is that the HOMO and LUMO energy levels are largely localized on the donor moiety and the acceptor moiety, respectively (though HOMO is more delocalized along the D−A structure).[33,59] This feature offers an important advantage of *individually* tuning the band gap and energy levels of the conjugated polymer. For example, a smaller band gap can
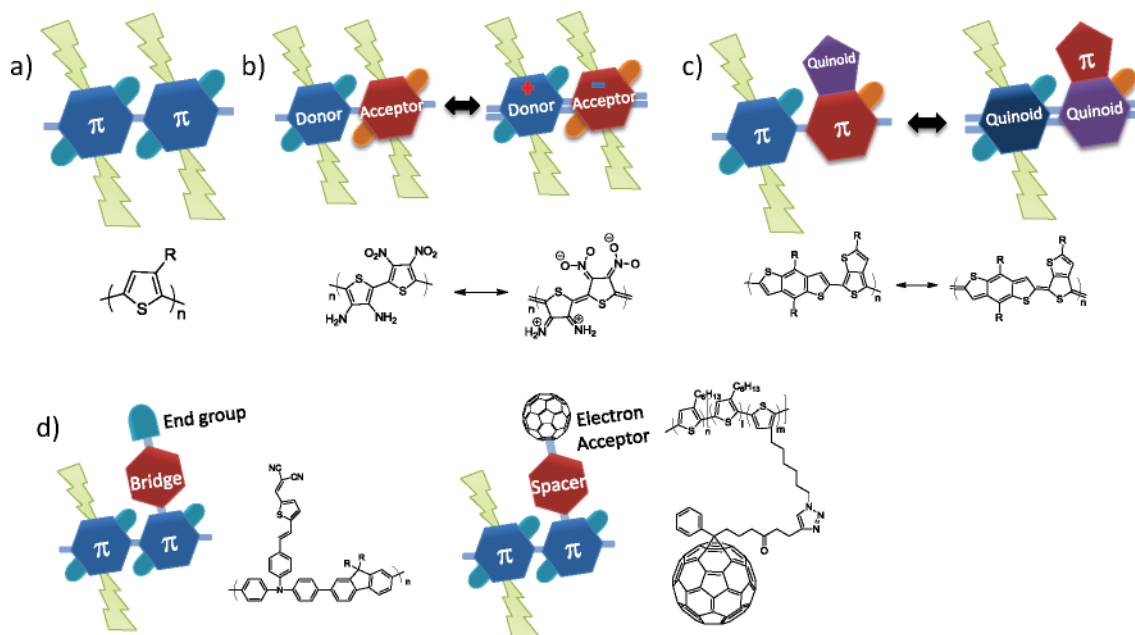
Figure 3. Different types of conjugated polymers with representative structures: (a) homopolymer; (b) donor–acceptor polymer; (c) quinoid polymer; (d) other types.

be obtained by copolymerizing a more electron-rich donor moiety and a more electron-deficient acceptor moiety, whereas the HOMO and LUMO levels can also be adjusted by varying the electron-donating ability of the donor moiety and the electron affinity of the acceptor moiety.[59] Most of the conjugated polymers for PSC reported so far are based on this D–A concept, with several of them showing over 7% efficiency in their BHJ cells.[45,60–63]

"Quinoid" polymers employ a different approach to effectively lower the band gap. Typically two aromatic units are fused in a particular geometry to take advantage of the larger value of resonance energy of the first aromatic unit (e.g., benzene, 1.56 eV) over the second unit (e.g., thiophene, 1.26 eV), so that the second aromatic unit (e.g., thiophene) tends to dearomatize to adopt a quinoid structure. Since the quinoid resonance form is lower in energy than the aromatic form, stabilizing the quinoid form will effectively reduce the band gap of related conjugated polymers. Figure 4 shows a few successful
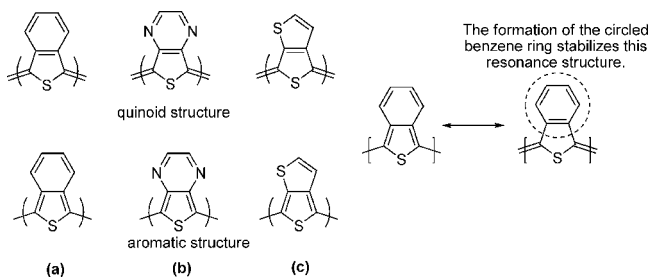
Figure 4. Aromatic and quinoid forms of poly(benzo[c]thiophene) (a), poly(thieno[3,4-b]pyrazine (b), and poly(thieno[3,4-b]thiophene) (c). Reprinted with permission from ref 7. Copyright 2010 American Chemical Society.

examples, including poly(benzo[c]thiophene) (E_g = 1.1 eV),[64] poly(thieno[3,4-b]pyrazine) (E_g = 0.95 eV),[65] and poly(thieno[3,4-b]thiophene) (E_g = 0.8–0.9 eV).[66,67] The major drawback of these fused systems lies in their relatively high-lying HOMO energy levels, which explains that low-band-gap copolymers synthesized by

alternating these prequinoid monomers with other aromatic rings such as thiophenes and fluorenes showed low V_{oc} in BHJ solar cells.[68–73] Further engineering the substituents on these conjugated backbone can lower the HOMO levels,[74–77] thereby leading to impressive efficiency numbers (over 7%).[74,78]

Rather than inserting electron-deficient acceptor moieties into the conjugated backbone to lower the band gap, the bridge polymer attaches them as the pendant groups to the backbone, aiming to optimize the absorption and conserve/promote the isotropic charge transport without any interruption by these acceptor moieties.[79,80] There are only a few examples of these bridge polymers with limited success.[79–81] One challenge for this type of polymers is the understanding and control of the active layer morphology.

The so-called "double-cable" approach was designed with the hope of "building in" well-defined nanostructure/morphology, rather than going through an arduous struggle in controlling the morphology in typical BHJ cells of polymer/fullerene blends. This "double-cable" design covalently links electron acceptors such as fullerenes (ACCEPTOR cable) to electron DONORS such as the conjugated backbones (DONOR cable). The advantages of this design include (i) a larger DONOR–ACCEPTOR interfacial area when compared with a typical BHJ structure, (ii) absence of undesirable large phase separation, (iii) relatively stable morphology, and (iv) variation of the chemical structures of the DONOR and the ACCEPTOR and length of the spacer between them, allowing to fine-tune the electronic interaction among the double-cable components.[82,83] Several materials of this "double-cable" design have been demonstrated in polymer solar cells.[84–89] However, the PCE of such devices is still at a very low level, likely due to fast recombination of opposite charges, ineffective interchain charge transport, and low ACCEPTOR content.[90,91]

Because of the aforementioned advantages, the versatility in design, and the popularity of the D–A polymers, *we will focus on the design of donor–acceptor polymers in this Perspective.*

2.3. A "Weak Donor–Strong Acceptor" Approach toward Ideal Polymers. As discussed in section 1.3, the ideal

conjugated polymer for BHJ solar cells should have a low-lying HOMO energy level to ensure a high V_{oc} and a narrow band gap to maximize the J_{sc}. Because the D−A polymers offer the unique feature of almost independently tuning the energy levels and the band gap, a "weak donor–strong acceptor" strategy has been proposed to maintain a low HOMO energy level via the "weak donor" and to result a narrow band gap by employing a "strong acceptor" via ICT (Figure 5).[59] In addition, the charge
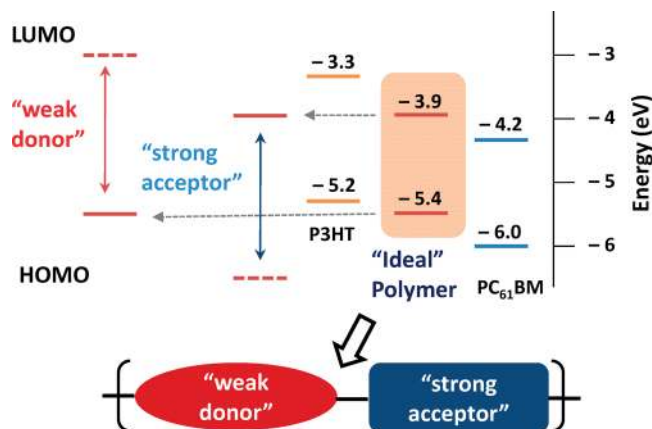

Figure 5. "Weak donor–strong acceptor" concept and energy levels. Adapted with permission from ref 59. Copyright 2010 American Chemical Society.

mobility, molecular interaction, and stability of a conjugated polymer can also be optimized by appropriate backbone design.

In the following sections, we will categorize various electron-donating units and electron-accepting units from the literature based on their structural features. The goals are to (a) summarize structure–property relationships of these units, and (b) identify principles that can facilitate future designs.

2.3.1. Selection of Donor Units. To design a suitable donor unit, first and foremost is to control its electron-donating ability, which has a large impact on the HOMO level and the band gap of conjugated polymers. Fused conjugated units are generally employed, since an appropriate fusion of a few single aromatic units can not only tune the electronic properties but also impact the charge mobility and intermolecular interactions of related conjugated polymers.

2.3.1.1. Fused Three Rings: Control over the Energy Levels. Figure 6a summarizes a few fused conjugated units with three rings. For example, fluorene is one of the most popular donor units used in D−A polymers for PSC due to a few notable features of the polyfluorenes, such as good thermal and chemical stability, high charge carrier mobility, and high absorption coefficients. In addition, the synthesis and alkylation of fluorene unit are readily accessible.[95−98] Furthermore, the central fused five-membered ring structure of the fluorene eliminates the otherwise severe steric hindrance of adjacent benzene units. Also, the alkyl chains are usually anchored on the 9-position of the fluorene, which does not add any
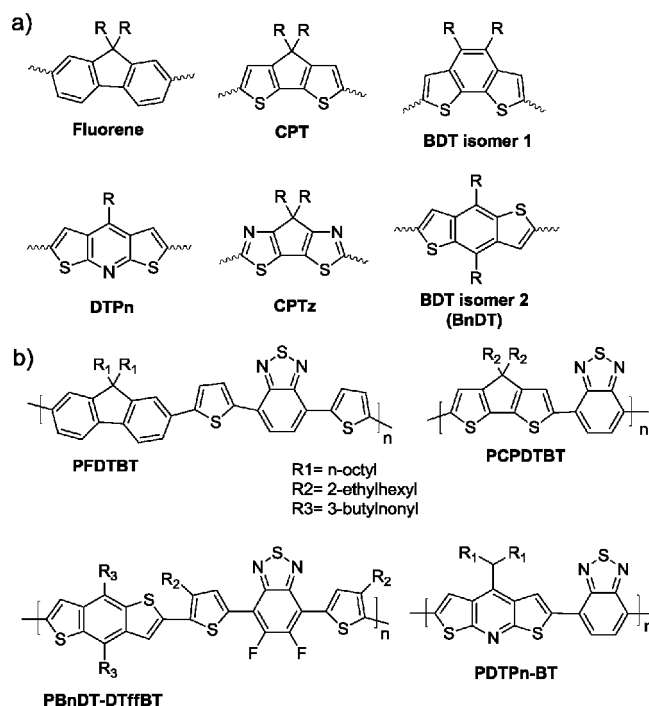
Figure 6. (a) Examples of fused-three-ring donor units. (b) Chemical structures of related copolymers.

additional steric hindrance. All these lead to a planar backbone of fluorene-related conjugated polymers, improving the intermolecular interaction and stacking of conjugated polymers.

Electronically, the fluorene unit is a very weak electron donor because of the relatively electron-deficient benzene units.[99] Therefore, most fluorene-based conjugated polymers have low HOMO levels around −5.5 eV.[74,100−103] As a result, V_{oc} of polyfluorene-based BHJ solar cells are generally around 1 V (Table 1).[100,102] However, these polymers usually have relatively large band gaps, which are not ideal for efficient light harvesting. To address this band-gap challenge, the thiophene analogue of the fluorene, cyclopentadithiophene (CPT) unit by fusing two thiophene units, was developed.[104] The CPT unit is much more electron-rich than the fluorene; thus, the ICT between the CPT donor unit and the acceptor unit is much stronger, leading to a significantly decreased band gap of related polymers (e.g., 1.4 eV).[104−106] The J_{sc} of CPT-based polymers can reach up to ∼17 mA/cm² by optimizing the morphology with additives, which is among the highest J_{sc} in polymer solar cells.[5,93] Unfortunately, the electron-rich nature of the CPT raises the HOMO of CPT-based polymers to around −5.2 eV; therefore, a small V_{oc} is generally observed (0.5−0.6 V).

Comparison between the fluorene and the CPT leads to the conclusion that a weak donor with electron-donating ability in between CPT and fluorene would be desirable toward the ideal polymer of both a low HOMO energy level and a narrow band gap. One natural choice is to fuse the benzene unit and the thiophene unit, such as the BDT unit (and its isomers). Both

Table 1. Summary of Band Gaps, HOMO Levels, and Photovoltaic Properties of Conjugated Polymers in Figure 6b

polymer	band gap (eV)	HOMO (eV)	V_{oc} (V)	J_{sc} (mA/cm²)	FF	PCE (%)	ref
PFDTBT	1.9	−5.7	1.04	4.66	0.46	2.2	92
PCPDTBT	1.4	−5.3	0.62	16.2	0.55	5.5	93
PBnDT-DTffBT	1.7	−5.5	0.91	12.91	0.61	7.2	61
PDTPn-BT	2.1	−5.6	0.31	0.75	0.37	0.09	94

a)

Fluorene　　Silafluorene　　Carbazole　　Germafluorene

CPT　　Silol bithiophene　　Dithienopyrrole　　Dithienogermole

b)

X= C　C-PCPDTBT
X= Si　Si-PCPDTBT

PSiF-DBT

PDTP-DTDPP

R1= n-dodecyl
R2= n-octyl
R3= 2-ethylhexyl
R4= n-butyl

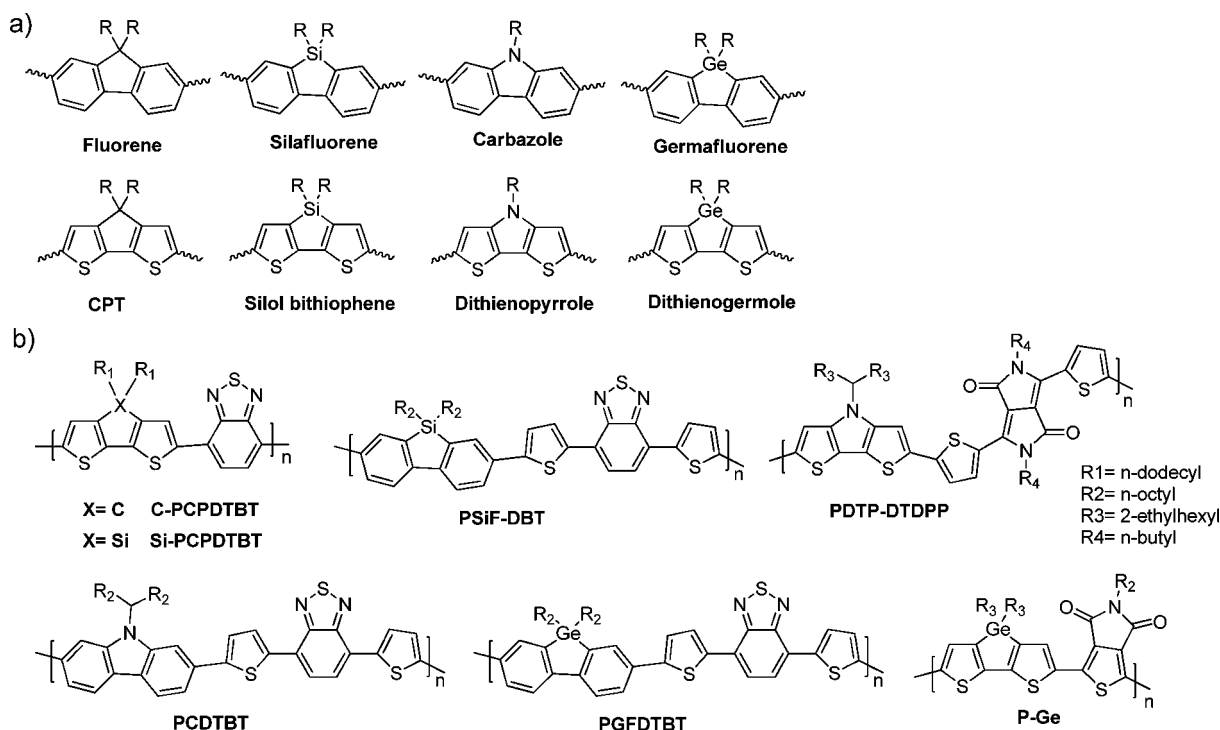PCDTBT　　　　　PGFDTBT　　　　　P-Ge

Figure 7. (a) Structures of donor units fused by bridging atoms. (b) Chemical structures of related copolymers.

Table 2. Summary of Band Gaps, HOMO Levels, and Photovoltaic Properties of Conjugated Polymers in Figure 7b

| polymer	band gap (eV)	HOMO (eV)	V_{oc} (V)	J_{sc} (mA/cm^2)	*FF*	PCE (%)	ref
Si-PCPDTBT	1.4	−5.3	0.57	17.3	0.61	5.9	5
C-PCPDTBT	1.3	−5.3	0.37	15.5	0.48	2.7	5
PSiF-DBT	1.82	−5.4	0.90	9.5	0.51	5.4	109
PDTP-DTDPP	1.13	−4.90	0.38	14.87	0.48	2.7	110
PCDTBT	1.9	−5.5	0.88	10.6	0.66	6.1	4
PGFDTBT	1.8	−5.6	0.79	6.9	0.51	2.8	111
P-Ge	1.69	−5.6	0.85	12.6	0.68	7.3	62

BDT isomers have a benzo core in the center and two flanking thiophene rings. BDT units offer two advantages: the necessary alkylation (to improve the solubility of resulting polymers) can be fulfilled on the center benzene ring, and the two flanking thiophene units render much less steric hindrance with adjacent acceptor units, leading to a more planar backbone. The differences of the isomers are on the linking position of these three subunits and symmetry of the molecule (to be discussed later in section 2.3.1.4). Both of the isomers exhibit weaker electron-donating ability compared with that of the CPT. Therefore, the HOMO levels of some BDT-based polymers are closer to the ideal HOMO energy level.[6,45,61,107] Together with a relatively narrow band gap, a few BDT-based polymers have demonstrated PCE over 6% in their BHJ cells.[45,61,107] Particularly, BHJ PV devices based on PBnDT-DTffBT has been shown with a V_{oc} around 0.9 V and a J_{sc} over 12 mA/cm^2, leading to a PCE over 7%.[61]

Further decreasing of electron-donating ability of the donor unit can be realized by changing the benzo unit to the pyridine unit or switching thiophene units to thiazole units as exemplified in Figure 6. Polymers based on both of the units show significantly decreased HOMO levels.[94,108] However, dithienopyridine (DTPn)-based polymers exhibit decreased V_{oc} along with decreased J_{sc} due to their larger band gaps. Possible

reasons are non-ideal polymer—PC$_{61}$BM interaction and poor exciton dissociations.[94]

Further tuning of the electron-donating ability and other physical properties of these donor units can be achieved via modifying specific atoms of the donor units (Figure 7 and Table 2).

Replacing the center (the only sp^3) carbon atom of the CPT unit with silicon has been thoroughly studied by Brabec and co-workers.[112,113] Since carbon and silicon have similar electron negativity and outer layer electronic structure (s^{2}p^2), CPT and silol dithiophene have a similar electron-donating ability. This explains the fact that HOMO levels and band gaps of the Si-bridged polymer (Si-PCPDTBT) and the C-bridged polymer (PCPDTBT) are nearly identical. However, the larger silicon atom and the longer C—Si bond modify the geometry of the fused dithiophene unit, allowing a better stacking of the polymer backbone. This helps improve hole and electron mobilities of Si-PCPDTBT/PC$_{71}$BM blend, a factor of 2—3 higher than those of the PCPDTBT/PC$_{71}$BM blend. Further indication for the better stacking of Si-PCPDTBT can be found from the absorption spectra of polymer thin films. In spite of similar band gaps between Si-PCPDTBT and PCPDTBT, a strong aggregation peak is present around 750 nm in the case of Si-PCPDTBT. This is confirmed by grazing incidence X-ray study (Figure 8). A pronounced diffraction peak at 5.2° (17 Å), typical for alkyl chains separating the backbones, and a weak
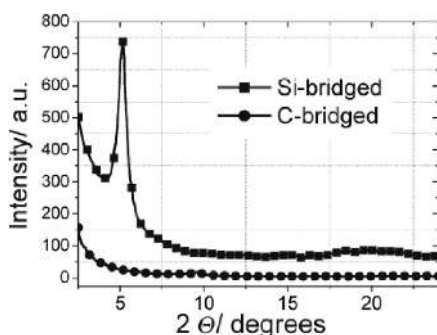
Figure 8. Diffractometry images of films of pristine silicon-bridged (squares) and carbon-bridged polymer deposited on quartz substrates. Reprinted with permission from ref 112. Copyright 2010 Wiley-VCH Verlag GmbH & Co. KgaA.

peak at around 20° corresponding to the backbone $\pi-\pi$ stacking are observed in thin films of Si-PCPDTBT. These data support a much ordered stacking of backbone and side chains of Si-PCPDTBT. Importantly, this enhanced aggregation reduces the formation of charge-transfer complexes[114] and increases the formation of free charge carriers. Thus, this seemingly small change from carbon to silicon leads to pronounced increases on both the V_{oc} (from 0.37 to 0.57 V) and the J_{sc} (from 15.5 to 17.3 mA/cm^2) under the same processing condition, with a PCE of 5.9% achieved for Si-PCPDTBT (vs 2.7% for PCPDTBT).[5]

However, changing the bridging atom of the fluorene from carbon to silicon has a strong effect on the electron-donating ability and energy levels of related polymers (PFDTBT vs PSiF-DBT).[109] Furthermore, silafluorene-based polymers have higher electroluminescent efficiency, thermal stability, and slightly larger hole mobility.[115] Therefore, a larger J_{sc} has been demonstrated with a little drop on V_{oc}, and a PCE over 5% has been realized for a silafluorene-based polymer.[109]

On the other hand, pyrrole is much more electron-rich than the cyclopentadiene (the center structural unit of the CPT). By replacing the bridging carbon atom of the CPT unit with a nitrogen atom, the resulting dithienopyrrole unit should have a stronger electron-donating ability than that of the CPT.[116] This leads to a more pronounced ICT between the dithienopyrrole and the acceptor unit; therefore, a decreased band gap is generally observed for dithienopyrrole-based polymer when compared with those of CPT-based D−A polymers. The FET mobility of dithienopyrrole-based polymers is slightly increased due to an enhanced polymer chain planarity and chain−chain interaction.[117] However, because of the electron-rich nature of the dithienopyrrole, the HOMO levels of dithienopyrrole-based polymers are elevated to around 5.0 eV,[110,116,118] which would lead to significantly decreased V_{oc} and environmental instability of related solar cells. In addition, since only one side chain is allowed on the N atom, a long and bulky alkyl chain is required to render reasonable solubility in common organic solvents. In general, these long and bulky side chains have negative impacts on the PV properties (further discussion will be provided in section 2.5.2). Nevertheless, a high J_{sc} of 14.87 mA/cm^2 and a respectable total efficiency of 2.7% were demonstrated for a dithienopyrrole-based polymer in its BHJ solar cells with PC$_{71}$BM, despite a V_{oc} of just 0.4 V.[110]

However, substituting the center carbon in the fluorene unit with a nitrogen (i.e., converting the fluorene into the carbazole) received more success for a number of reasons. First, since

fluorene unit itself is relatively electron-deficient (compared with the CPT), the addition of an electron-donating nitrogen would slightly increase the electron density of the resulted carbazole unit. Therefore, the HOMO energy levels of carbazole-based D−A polymers would increase, closer to the ideal HOMO level (Figure 5). Second, the polycarbazoles have been successfully used in polymer LED[119] and FET,[120] demonstrating excellent p-type transport properties. Third, the carbazole unit is fully aromatic and not too electron rich, offering a decent chemical and environmental stability.[121] Therefore, it is not surprising that a carbazole-based polymer (PCDTBT) has been demonstrated with a V_{oc} of 0.88 V, a J_{sc} of 10.6 mA/cm^2, and an impressive FF around 66%, leading to an overall PCE over 6% in its BHJ cells with PC$_{71}$BM.[4]

Other hetreoatoms have also been explored as the bridging atoms (Figure 7). For example, germafluorene-containing polymers have been reported.[111] Germanium is in the same group (group 14 on the periodic table) with C and Si, but with a larger radius. The optical band gap and the HOMO level of polygermafluorene are similar to those of poly(silafluorene)s, indicating a similar electron-donating ability of the germalfluorene. Interestingly, polymers based on germafluorene do not show as good PV performance as poly(silafluorene)s, largely because of a decreased V_{oc}, in spite of lower HOMO levels than these of poly(silafluorene)s. Similarly, dithienogermole with Ge as the bridging atom was also reported by Amb et al.[62] Similar energy levels and band gaps were reported for silol−dithiophene- and dithienogermole-based copolymers. Both copolymers exhibit great photovoltaic properties with PCEs over 6% in inverted BHJ solar cells with PC$_{71}$BM as the acceptor.

2.3.1.2. High Level of Fusion: Ladder Type Donors. Inspired by the success of fused three rings, high level of fusion of the aromatic units on the conjugated backbone has also been actively explored because it can facilitate π-electron delocalization to increase the effective conjugation length, offering an effective method to reduce the band gap, in addition to controlling energy levels (Figure 9).[122,123] Moreover, the resulting coplanar geometries and rigid structures can suppress the rotational disorder around interannular single bonds and lower the reorganization energy, which in turn can enhance the charge mobility.[124−126] This high level of fusion can be achieved by either covalently fastening adjacent aromatic units in the backbone (i.e., ladder type) or by fusing three or more aromatic units into an enlarged conjugated π unit. However, excessively strong interchain $\pi-\pi$ stacking interactions arising from this high degree of coplanarity could make the conjugated polymers insoluble and unprocessable.[127]

For example, the poly(fluorene) and the poly(CPT) discussed above can be considered as fused poly(phenylene) and poly(thiophene), respectively. Besides the benefits such as band gap reduction and charge mobility enhancement, the symmetry of these alkylated fused thiophene units eliminates any possible regioregularity issue of poly(3-alkylthiopene)s, which could decrease effective π-conjugation of the conjugated backbone.[53,54]

The higher level of fusion can help increase environment stability of related polymers and fix possible isomerization of conjugated polymer backbones. For example, in the poly(phenylenevinylene) (PPV), the photo-oxidation via [2 + 2] cycloaddition of excited-state singlet oxygen and vinylene group would result in an irreversible chain scission with consequent reduction of the conjugation length and a blue-shifted absorption.[130,131] To address the issue of the easy oxidation of the vinyl linkage, Song et al. cyclized the vinylene group with
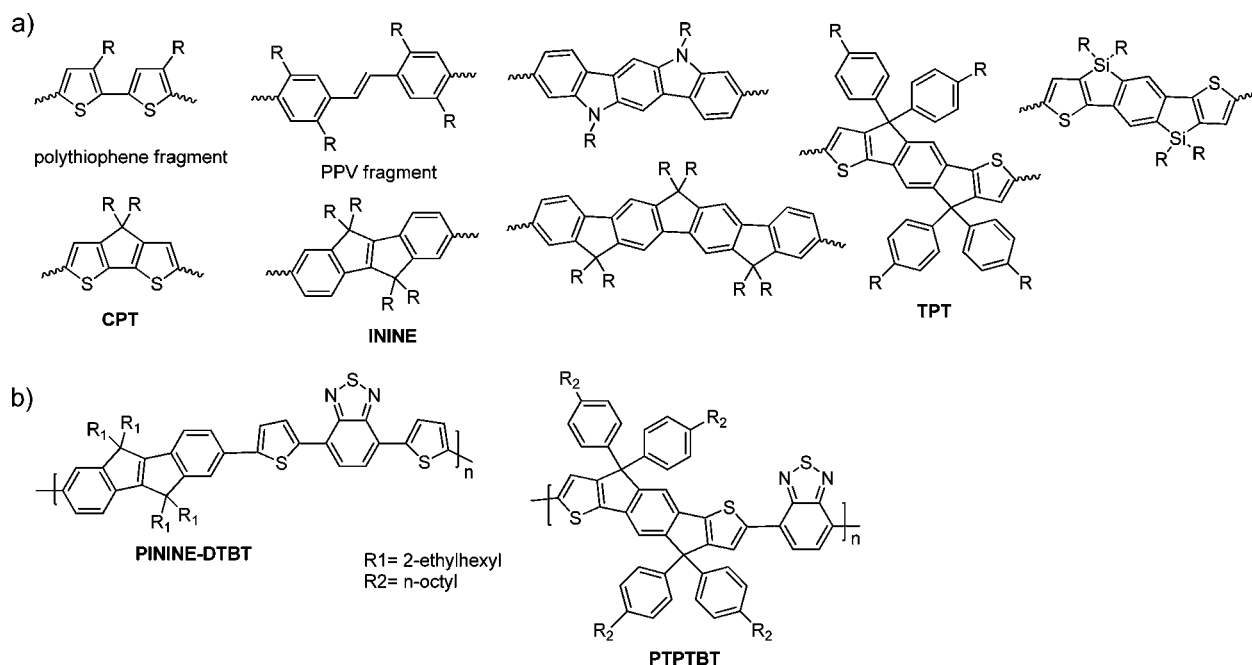
Figure 9. (a) Chemical structures of ladder-type donor units. (b) Chemical structures of related copolymers.

Table 3. Summary of Band Gaps, HOMO Levels, and Photovoltaic Properties of Conjugated Polymers in Figure 9b

polymer	band gap (eV)	HOMO (eV)	V_{oc} (V)	J_{sc} (mA/cm^2)	FF	PCE (%)	ref
PININE-DTBT	1.84	−5.45	0.47	5.93	0.43	1.88	128
PTPTBT	1.57	−5.36	0.85	11.2	0.67	6.41	129

adjacent benzene units using two 5-membered rings with carbon as the bridge.[128] This conversion of PPV into ININE copolymers would prevent backbone scission by singlet oxygen. Thus, polymers containing ININE show significantly enhanced UV−vis and PL stability after irradiation with white light in air.

More ladder-type donor units by fusing three or more adjacent units have been developed (Figure 9).[43,132−138] In addition to the advantages mentioned above for these fused systems, these ladder-type systems may additionally lead to broader, more intense absorption bands which will result in enhanced solar light harvesting. Furthermore, for every repeating unit in the ladder-type donor containing polymers, there are more positions to attach solubilizing chains, which may provide a better solution processability of the related polymers.[43] Some typical ladder-type donor units are summarized in Figure 9. All the constructing subunits are just benzene and thiophene rings. With different bridging atoms, the electronic properties of these ladder-type donors can be adjusted as discussed above. The highest PCE over 6% with a high V_{oc} of 0.85 V has been achieved by a conjugated polymer containing ladder-type donor unit TPT with a low HOMO level of 5.36 eV (Table 3).[129]

2.3.1.3. High Level of Fusion: Fused Conjugation over Three or More Aromatic Units. Another method to achieve the high level of fusion is to fuse three or more aromatic units into an enlarged conjugated unit with extended π-conjugation (Figure 10). Similar to ladder type systems, these extended π-conjugation systems feature enforced planarity and more effective π-electron delocalization, which can lead to broader light absorption and improve π−π interactions between polymer chains in thin solid films to enhance the charge carrier mobility.[140] In addition, the HOMO energy levels of

related polymers can be tuned through adjusting the fused aromatic moieties within these polycyclics.

For example, replacing the benzene core of benzodithiophene (BDT isomer 1) with a more electron-deficient naphthalene core leads to the naphthalenedithiophene (NDT isomer 1). NDT-based polymers exhibit both small band gaps and low HOMO levels.[141] Noticeably, a NDT-based polymer (PNDT-DTPyT) exhibited a large J_{sc} of 14.16 mA/cm^2 and a decent V_{oc} of 0.71 V, with a PCE of 6% in its BHJ solar cells (Table 4).[107] To further decrease the electron-donating ability of the donor unit for a deeper HOMO level, dithienoquinoxaline (QDT) with a more electron-deficient quinoxline core was designed. Indeed, QDT-based polymers exhibited enhanced V_{oc}, but smaller J_{sc}, in related BHJ solar cells due to decreased HOMO levels but concomitantly larger band gaps when compared with those of NDT analogues.[46,107,141] In another example, quadrathienonaphthalene (QTN) with an even larger pancake-like π-conjugation prompts better electron delocalization, molecular interaction, and hole mobility. Therefore, the QTN-based polymers exhibit smaller band gaps and slightly decreased HOMO levels. The homopolymer of QTN has a band gap of 2.0 eV, and an efficiency over 2% was demonstrated.[139]

Besides cyclic extension of the conjugation, linear extension on the donor unit has also been explored to adjust energy levels and enhance molecular interaction and charge mobility. However, there are only a few reported cases due to synthetic difficulties of these units (structures on the second row of Figure 10a).[142−146] Further, it is quite a challenge to attach solubilizing chains on these linearly extended aromatic systems. Nevertheless, some unique properties of this type of donor units do exist. For example, these donor units have very stiff backbones, long

Table 4. Summary of Band Gaps, HOMO Levels, and Photovoltaic Properties of Conjugated Polymers in Figure 10b

polymer	band gap (eV)	HOMO (eV)	V_{oc} (V) exp	J_{sc} (mA/cm^2)	FF	PCE (%)	ref
PNDT-DTPyT	1.53	−5.36	0.71	14.16	0.62	6.2	107
PQDT-DTPyT	1.56	−5.50	0.75	13.49	0.55	5.6	107
HMPQTN	2.00	−5.39	0.72	5.69	0.50	2.06	139

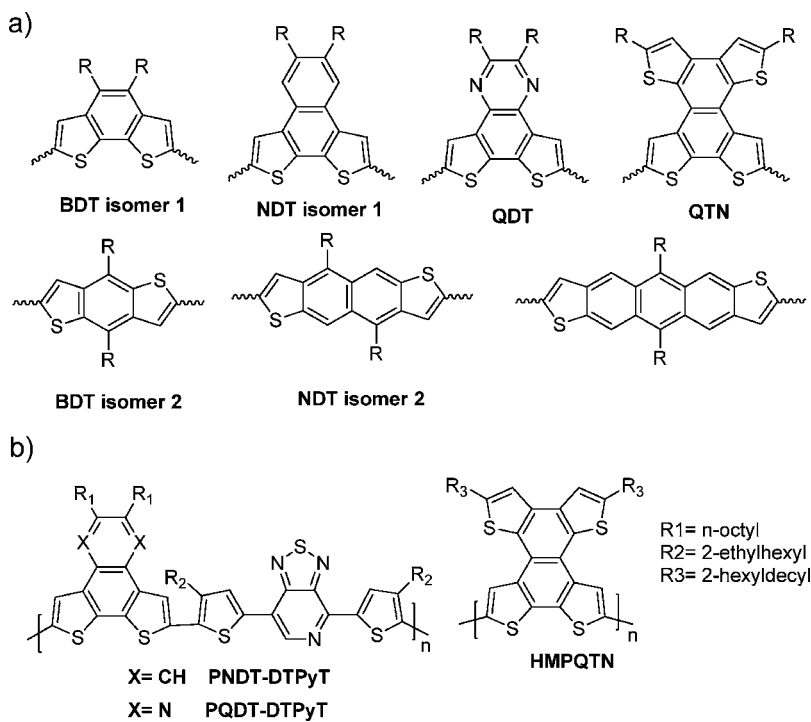**Figure 10.** (a) Chemical structures of polyaromatic donor units. (b) Chemical structures of related copolymers.

effective π-conjugation length, good environment stability, and moderate electron-donating properties. They usually have strong π-stacking, which allows effective overlap of π-orbitals; thus, they are good candidates for OFET applications with excellent charge carrier mobilities. These high mobilities also render related polymers promising candidates for PSC. In addition, the distance between side chains can be adjusted by varying the number of (unalkylated) fused aromatics between alkylated ones, which allows tuning of the intercalation of $PC_{61}BM$.[147,148]

Interestingly, sometimes unfused rings offer additional advantages, especially when these unfused additional aromatic units are pendant to the conjugated backbone, without introducing steric hindrance to the backbones.[6,149] Figure 11
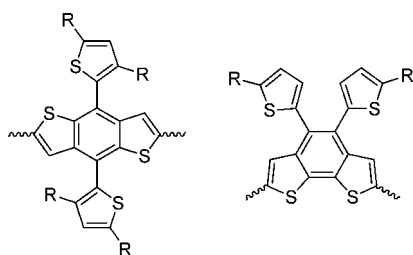

Figure 11. Chemical structures of donor units with aromatic side chains.

provides two such examples where these pendant thiophene units are not coplanar with the conjugated donor units on the

polymer main chain. However, these pendant thiophene units would prohibit excessive π-stacking of polymer backbones; thus, they can be used to adjust molecular interaction and active layer morphology. Reduced π-stacking would also lead to better solubility of the conjugated polymers. Unlike these insulating alkyl chains, these aromatic rings can potentially help the charge transport. In addition, polymers containing these unfused rings exhibit significantly increased V_{oc} in BHJ solar cells.[6,149] The same enhancement has also been reported in small molecule solar cells and systematically studied.[48]

2.3.1.4. Symmetry of Donor Units. As already alluded in the previous discussion, fused aromatics often lead to isomers. In this scenario, symmetry of the molecule plays an important role. Recent studies have indicated that symmetry of the monomers and the related curvature of the polymer chains have large impacts on HOMO levels and charge mobility of conjugated polymers.

A comprehensive investigation on the impact of the symmetry was recently completed with the linear- and angular-shaped naphthodithiophenes (NDTs) (Figure 12).[150,151] Takimiya et al. discovered that NDTs of angular shapes (NDT3 and NDT4) showed lower HOMO levels and larger band gaps than their linear counterparts (NDT1 and NDT2).[151] Interestingly, when it comes to the mobility, NDTs of centrosymmetry (NDT1, NDT3, and NDT4) have enhanced mobilities than that of the NDT of axis symmetry (NDT2). Further, NDT4 with sulfur atoms facing outward presumably has a larger intermolecular orbital overlap through sulfur-involved nonbonding contact than that of NDT3 with sulfur atoms embedded in the bay region, which explains the observed higher mobility of NDT4.
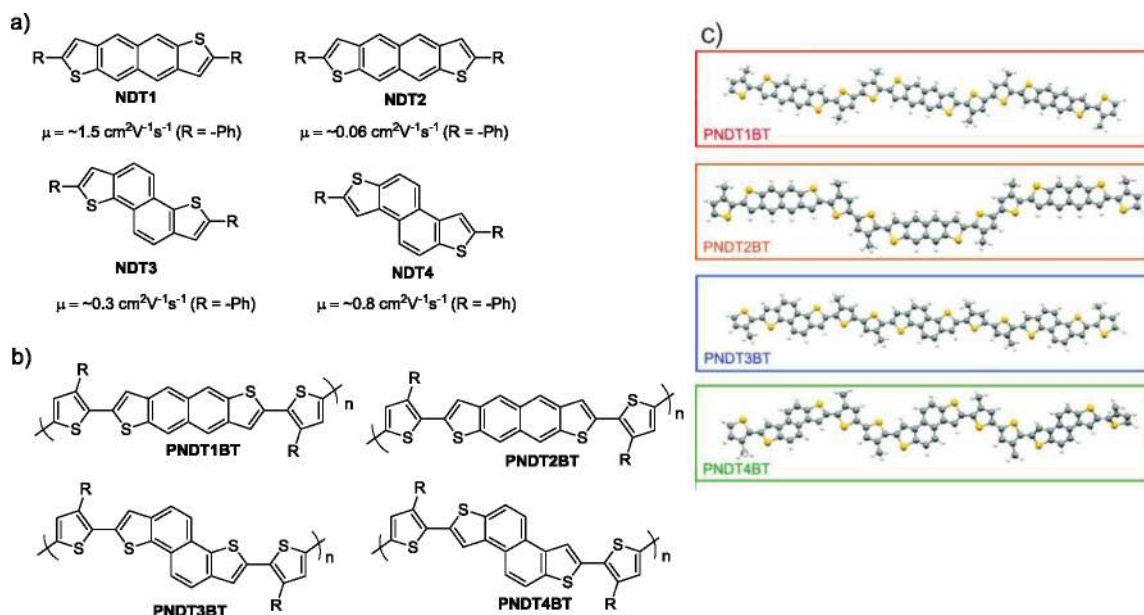
Figure 12. (a) Four isomeric naphthodithiophenes: naphtho[2,3-b:6,7-b′]dithiophene (NDT1), naphtho[2,3-b:7,6-b′]dithiophene (NDT2), naphtho[1,2-b:5,6-b′]dithiophene (NDT3), and naphtho[2,1-b:6,5-b′]dithiophene (NDT4). (b) Chemical structures of the naphthodithiophene-based semiconducting polymers. (c) Optimized backbone structures of the polymers PNDT1BT, PNDT2BT, PNDT3BT, and PNDT4BT. The side chains were replaced with methyl groups to simplify the calculation. Reprinted with permission from refs 150 and 151. Copyright 2011 American Chemical Society.

Lower HOMO levels are also observed in polymers containing angular-shaped NDTs. In addition, stacking of polymer chains is much stronger in polymers containing NDTs of centrosymmetry than in polymers with NDTs of axis symmetry. However, the mobility of polymers are affected by other factors than just the shape and symmetry of the donor unit (NDT).[150] A different mobility rank was summarized for these polymers containing NDT and two thiophene units (PNDT3BT > PNDT4BT > PNDT1BT > PNDT2BT). This difference in mobility rank between the polymers and NDT molecules can be related to the curvature of the backbone of these polymers. As shown in Figure 12, though NDT1 has a linear shape and NDT3 has an angular shape, the PNDT3BT could adopt a pseudostraight-shaped backbone (rather than a zigzag-shaped one in the case of PNDT1BT), which would lead to an effective packing of PNDT3BT into most highly ordered structure among all these four polymers, thereby the highest mobility. Similar results were reported by Müllen and co-workers, who also studied the impact of the shapes and curvature of the molecules on mobilities.[152,153]

To conclude this discussion on the donor units, Figure 13 shows an empirical electron-donating ability trend of representative donor units. This donor unit trend is based on the comparison of oxidation potentials and band gaps of polymers with identical acceptor units. Due to the influences of other factors, such as steric hindrance and significant differences on π-stacking, this trend may vary. Generally, a "weak donor" with moderate electron donating ability is needed to create polymers with ideal HOMO levels around −5.4 eV. High mobility, proper intermolecular interaction, enhanced π-electron delocalization, and bonding geometry also need to be taken into consideration in order to design high performance conjugated polymers.

2.3.2. Design of Acceptor Units. Similar to the donor units, the acceptor units are of equal importance in controlling the energy levels and band gaps of conjugated polymers. However,

compared with the great variety of donor units reported (e.g., a few successful examples discussed in previous section), the design and synthesis of functional acceptors only received moderate success. Nevertheless, several novel acceptor units have been developed, which contributed significantly to the enhanced photovoltaic performance of related polymers.

Perhaps the most commonly employed acceptor unit is the 2,1,3-benzothiadiazole (BT). Because of its strong electron-accepting ability and commercial availability, BT has been very popular in constructing low-band-gap conjugated polymers.[93,104,154] Moreover, these two N atoms in the thiadiazole ring could possibly form hydrogen bonding with adjacent units (e.g., the hydrogen atom on the thiophene ring), leading to a more planar backbone. With all these good features, many polymers with a BT acceptor unit have shown low band gaps and good photovoltaic properties.[5,104,154] The best example comes from a conjugated polymer copolymerizing dithienosilole (Si-PCPDTBT) with the BT unit, which exhibited a band gap of 1.37 eV and thereby a J_{sc} of 17.3 mA/cm^2, with a PCE up to 5.9% in its BHJ devices.[5]

Adding one thienyl group on both sides of the BT converts BT into di-2-thienyl-2,1,3-benzothiadiazole (DTBT) (Figure 14),[4,41,42,109,155−157] which has a few more advantages when compared with the original BT unit. First, the two flanking thienyl units relieve the otherwise possibly severe steric hindrance between the BT unit and donor aromatic units (especially when benzene based aromatics are used).[128] Thus, the synthesized donor−acceptor polymers adopt more planar structures, thereby reducing the band gap by enhancing the D−A conjugation. In addition, a more planar conjugated backbone facilitates the chain−chain interactions among polymers in the solid state, improving the charge carrier (usually hole) mobility. Second, while the electron-accepting BT unit maintains the low band gap, the two electron-rich, flanking thienyl units would help improve the hole mobility, since thiophene-based polymers (such as P3HT) have shown noticeably high hole mobility.[158] Third, the
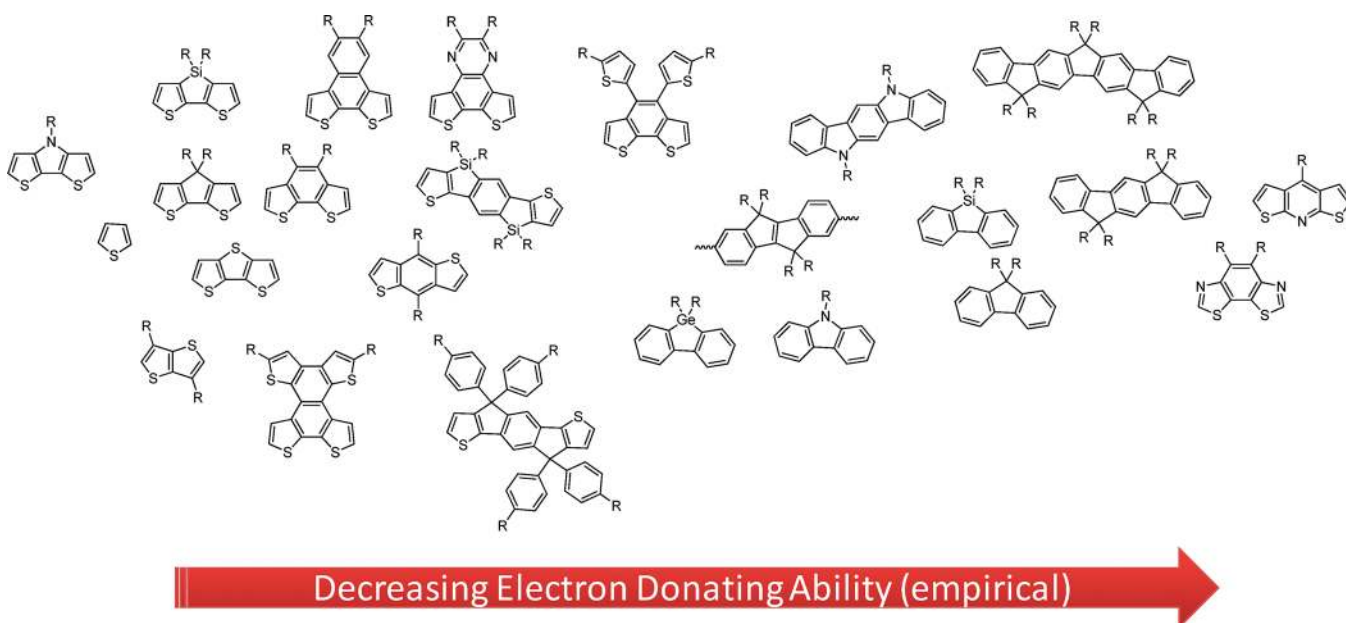
Figure 13. An empirical chart showing the relative electron-donating ability of various donor units.
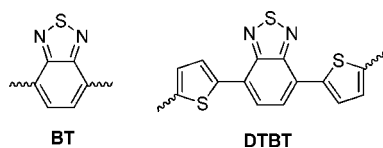
Figure 14. Chemical structures of BT and DTBT acceptor units.

BT unit has limited positions for addition of solubilizing chains or substituents, and attaching these units would likely introduce steric hindrance. To this end, these flanking thienyl units can provide more possible positions for further modification of electronic properties and solubility of conjugated polymers, with minimal steric hindrance involved if properly introduced.[159] However, due to the electron-rich nature of these thienyl units, in some cases, the two flanking thienyl units slightly increase the HOMO levels of the conjugated polymers when compared with BT-based polymers.[128,132]

Similar to the design of donor units (Figure 7), the electron affinity of acceptors can also be fine-tuned by varying specific atoms. Figure 15 lists a series of such units which can be treated as structurally related with the BT. For example, replacing the sulfur atom of the BT unit with a nitrogen atom, the electron-accepting ability of the triazole is significantly reduced when compared with that of the BT. It is because the lone pair on the middle nitrogen atom of the triazole unit is more basic than the lone pairs on the sulfur of the BT and is more easily donated into the triazole ring, making it relatively electron-rich when compared with the original BT. Thus, conjugated polymers incorporating triazole unit usually show a larger band gap around 2.0 eV (Table 5).[45] On the other hand, the electron-accepting ability of the quinoxaline (Qx) is in between the triazole and BT. One advantage of Qx is that it can be alkylated to improve the solubility of conjugated polymers without introducing steric hindrance.[160] In addition, alkylated benzo units can be introduced to the periphery of the Qx instead of alkyl chains, which provides additional control to adjust molecular interactions and may increase V_{oc} and charge mobility.[161,162] Benzoxadiazole (BX), the oxygen containing analogue to the BT unit, has very similar electron-accepting

ability to that of BT. Thus, polymers containing the BX unit have very similar HOMO and LUMO levels to those of BT-based analogues. Interestingly, these BX-based polymers usually do not perform as well as these BT-based analogues, possibly due to lower mobilities of these BX-containing polymers.[106,156,163] Lastly, the selenium analogue of the BT unit, 2,1,3-benzoselenadiazole (BSe), demonstrates many interesting properties in photoelectronic devices.[160,164] In general, BSe-based polymers exhibit smaller band gaps and lower HOMO and LUMO levels (from CV).[69,165,166] However, the photovoltaic properties of BSe-based polymers are restricted by the weak absorption of the active layer and the imbalance in the hole and electron transport of the active layer which may result from bad morphology.

In most of the high performance D−A conjugated polymers reported, close to ideal HOMO energy levels were achieved (e.g., −5.4 eV), which lead to an observed open-circuit voltage (V_{oc}) as high as 0.92 V.[6,45,61] However, very often the band gaps of these materials are still larger than the proposed 1.5 eV of ideal polymers, resulting in mediocre short-circuit currents (J_{sc}). In order to further improve the efficiency, a smaller band gap is needed to achieve a higher J_{sc} while the low HOMO energy level should still be maintained (for a high V_{oc}). According to the proposed approach of "weak donor−strong acceptor", one should incorporate "strong acceptors" with large electron deficiency in the conjugated backbone to lower the LUMO levels, thereby decreasing the band gap of related polymers. We will elaborate on this concept by discussing several such strong acceptors.

One such example is the dithienylthiadiazolo[3,4-c]pyridine (DTPyT), which differs from the original DTBT by only one atom (Figure 16). Compared with benzene, pyridine is π-electron deficient. Therefore by replacing the benzene in the BT unit with pyridine, the new acceptor, thiadiazolo[3,4-c]-pyridine (PyT), would be one such stronger acceptor. Polymers incorporating DTPyT unit were first reported by Leclerc et al.,[156] and their PV performances were then enhanced up to 6.3% by You et al. (Table 6)[107] by copolymerizing with "weak donors" to adjust energy levels and attaching solubilizing chains

Table 5. Summary of Band Gaps, HOMO/LUMO Levels, and Photovoltaic Properties of Conjugated Polymers in Figure 15b

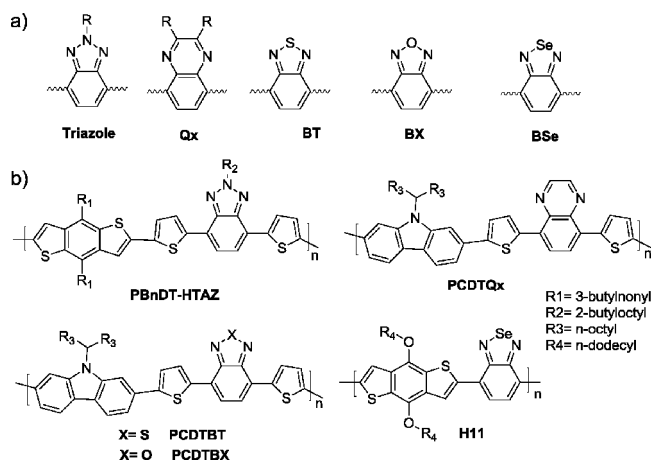| polymer	band gap (eV)	HOMO (eV)	LUMO (eV)	V_{oc} (V) exp	J_{sc} (mA/cm^2)	FF	PCE (%)	ref
PBnDT-HTAZ	1.98	−5.29	−2.87	0.70	11.14	0.55	4.30	45
PCDTQx	2.02	−5.46	−3.42	0.95	3.0	0.56	1.8	156
PCDTBT	1.88	−5.45	−3.60	0.86	6.8	0.56	3.6	156
PCDTBX	1.87	−5.47	−3.65	0.96	3.7	0.60	2.4	156
H11	1.52	−4.88	−3.33	0.55	1.05	0.32	0.18	69

Figure 15. (a) Chemical structures of trizole, Qx, BT, Bx and BSe units. (b) Chemical structures of related copolymers.

to improve the molecular weight and the film morphology. All the DTPyT-containing polymers reported by You and co-workers showed noticeably reduced LUMO levels, slightly reduced HOMO levels, and thus smaller band gaps than those of their DTBT counterparts. The smaller band gap significantly improves the observed J_{sc} of the related BHJ devices, while the low HOMO energy level maintains the high V_{oc}. Therefore all three polymers (PNDT-DTPyT, PQDT-DTPyT, and PBnDT-DTPyT) achieved high efficiency numbers in their BHJ devices, demonstrating the great utility of DTPyT acceptor moiety in designing high performance solar cell materials.

Similarly, tetrazine (Tz) which has a very high electron affinity has also been used as a strong acceptor to construct low-band-gap polymers with over 5% efficiency achieved.[167] When incorporated into D−A conjugated polymers, both HOMO and LUMO levels of Tz-based copolymers are lower than those of BT-based copolymers, indicating a stronger electron affinity of the Tz unit. Interestingly, the Tz unit shows more impact on HOMO levels than on LUMO levels, which is different from most acceptor units. This results in slightly broader band gaps of Tz-based polymers when compared with these of BT-based polymers.

Isoindigo is a symmetrical and perfect planar π-conjugated molecule consisting of two indolin-2-one units, which are strongly electron withdrawing.[168,170,171] A few conjugated polymers based on isoindigo units possess near-ideal low HOMO levels around −5.4 eV and low LUMO levels around −3.9 eV. However, relatively low PCE up to 3% was obtained, with a large V_{oc} of 0.9 V but a low J_{sc} around 5 mA/cm^2.[168] Further improvement can be anticipated by choosing proper donor units and side chains as well as by improving the active layer morphology.

Structurally similar to isoindigo, pyrrolo[3,4-c]pyrrole-1,4-dione (DPP) has also been used in a number of D−A conjugated polymers in the past 3 years.[1,44,118,169,172−176] Low

band gaps around 1.3 eV are generally obtained, which is beneficial for J_{sc}; however, HOMO levels of DPP-based polymers are significantly elevated when compared with those of their analogues with other acceptors, possibly due to these two flanking electron-donating thienyl units. Nevertheless, efficiency numbers as high as 5.5% were reported for DPP-based polymers.[169,176]

The thieno[3,4-c]pyrrole-4,6-dione (TPD) unit was recently intensively explored. The symmetric and planar structure of TPD could improve the electron delocalization, enhancing the polymer chain−chain interactions and increasing the hole mobility. Similar to DPP and isoindigo, electron-withdrawing amide groups render TPD a strong acceptor. It was first incorporated in BnDT-based copolymers by Leclerc and co-workers.[177] The resultant copolymer not only has a small band gap (thereby a potentially high J_{sc}), also maintains a low HOMO energy level of −5.56 eV. Therefore a high V_{oc} of 0.85 V was achieved in the BHJ device with PC$_{71}$BM as the acceptor. Along with a J_{sc} of 9.81 mA/cm^2 and a FF of 0.66, a PCE of ∼5.5% was obtained. It is particularly worth mentioning that Leclerc et al. obtained these impressive values from devices with an active area of 1.0 cm^2. Achieving high efficiencies on devices of large area is advantageous for real world application of PSC because efficiencies obtained on areas smaller than 0.2−0.3 cm^2 may become strongly substrate size-dependent, in addition to the possible overestimation of the J_{sc} from a very small area device. Similar polymers with identical conjugated backbone but having different solubilizing chains were independently reported by Jen's group and Xie's group with PCEs varying from 3.42% to 4.79% after certain optimization.[178,179] Fréchet and co-workers later did a detailed study on the impact of these side chains on the TPD−BDT copolymer.[180] PCEs up to 6.8% were reported just by varying the side chains of the conjugated backbone. More recently, TPD-based polymers of efficiency as high as 7.3% were reported by Amb et al. and Tao and co-workers.[60,62,63,181] In their studies, the TPD acceptor was copolymerized with fused bithiophene with different bridging atoms. All of these copolymers exhibit high PCEs over 6% in BHJ solar cells, which indicates a great potential of TPD unit in constructing novel materials for PSC.

However, acceptors should not be too electron withdrawing. As discussed earlier, the LUMO of the conjugated polymer should be at least 0.3 eV larger than the LUMO of the n-type material to facilitate efficient exciton dissociation. Too strong an acceptor in the D−A polymer would lead to too low a LUMO level and the inability to split excitons at the interface between the polymer and fullerenes. Thus, no photocurrent or extremely small J_{sc} would be observed. Several examples include benzo[1,2-c:4,5-c′]bis([1,2,5]thiadiazole) (BBTD),[182] [1,2,5]-thiadiazolo[3,4-g]quinoxaline,[183,184] pyrazino[2,3-g]quinoxaline,[185] and [1,2,5]thiadiazole[3,4-d]pyridazine.[186]

2.4. Substituents. Though the energy levels and band gap of a conjugated polymer are mainly determined by the selection of conjugated aromatic units (e.g., D and A in D−A polymers),

Table 6. Summary of Band Gaps, HOMO/LUMO Levels, and Photovoltaic Properties of Conjugated Polymers in Figure 16b

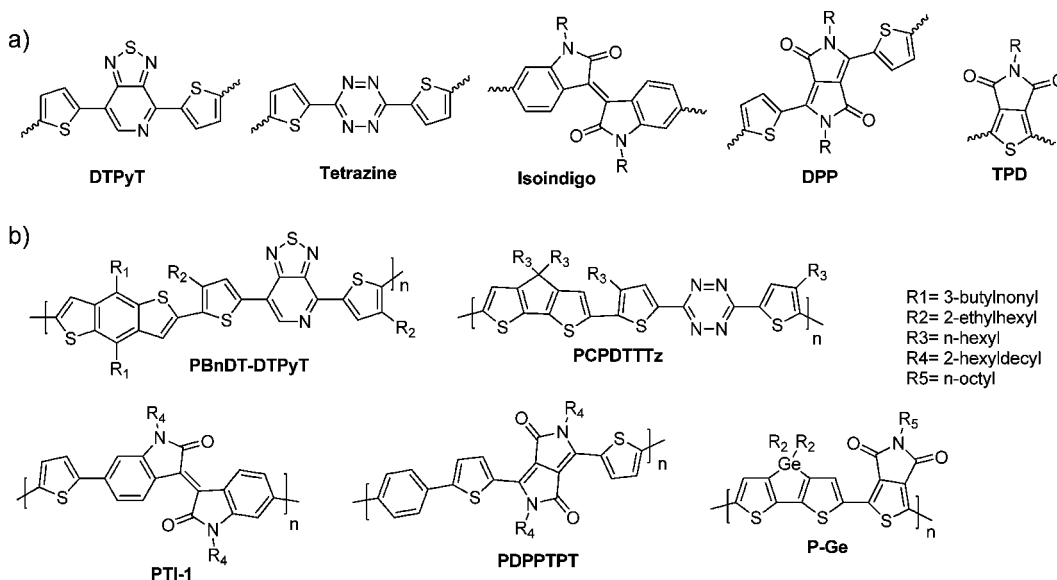| polymer	band gap (eV)	HOMO (eV)	LUMO (eV)	V_{oc} (V) exp	J_{sc} (mA/cm^2)	FF	PCE (%)	ref
PBnDT-DTPyT	1.51	−5.47	−3.44	0.85	12.78	0.58	6.3	107
PCPDTTTz	1.68	−5.34	−3.48	0.75	12.2	0.59	5.4	167
PTI-1	1.60	−5.85	−3.88	0.89	5.4	0.63	3.0	168
PDPPTPT	1.53	−5.35	−3.53	0.80	10.3	0.65	5.5	169
P-Ge	1.69	−5.6	NA	0.85	12.6	0.68	7.3	62

Figure 16. (a) Chemical structures of some "strong acceptor" units. (b) Chemical structures of related copolymers.

substituents can be used to further tune energy levels, band gaps, molecular interaction, and even morphology.

Using archetypical PPV as the model polymer, the substituent effect on conjugated polymers was systematically studied by Bredas and Heeger with the valence effective Hamiltonian (VEH) method (Figure 17).[187] Attaching
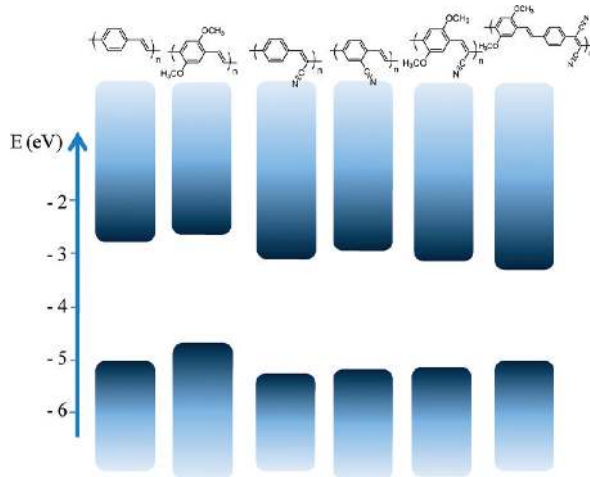
Figure 17. HOMO and LUMO of the compound investigated, relative to the work functions of calcium and aluminum.[187]

electron-donating methoxy groups to the benzene unit of the PPV would raise the HOMO energy level when compared with the original PPV (with similar LUMO level). This effect was also observed experimentally.[188] When switching to the electron-withdrawing group (such as cyano), stabilization on

both HOMO and LUMO levels would be expected. However, calculations found that the band gaps of the cyano PPVs would be larger than that of PPV because of the asymmetry in the stabilization of the HOMO and LUMO levels by the cyano substituent. Furthermore, the position of the cyano (either on the phenylene or on the vinylene) affects the energy levels and band gap. When cyano was added on the vinylene, the calculated LUMO level was noticeably lower than that of the analogue with cyano on the phenylene, with less difference on the HOMO energy levels. The authors attributed this effect to the different number of π-electrons on the vinylene and phenylene. Since vinylene unit only has two π-electrons whereas phenylene unit has six, substitution on the vinylene would introduce a relatively larger perturbation to the conjugated backbone, further lowering the LUMO level. All these results presented above indicate that electron-donating substituents (such as methoxy) would have a more significant impact on the HOMO level, while electron-withdrawing ones (such as cyano) would affect more strongly on the LUMO level. Therefore, by attaching both methoxy group and cyano group on the phenylene and the vinylene part of PPV, respectively, the resulting polymer exhibited a similar HOMO level with that of the methoxy PPV and a similar LUMO with that of the cyano PPV, leading to a significantly decreased band gap.[189] This result is in good agreement with the proposed "weak donor–strong acceptor" strategy to design ideal polymers.[59]

Another interesting substituent is the fluorine. Fluorine is the smallest electron-withdrawing group with a van der Waals radius of 1.35 Å and a Pauling electronegativity of 4.0. Fluorinated organic molecules exhibit a series of unique features such as great thermal and oxidative stability,[190] elevated resistance to degradation,[191] enhanced hydrophobicity, and

high lipophobicity in perfluorinated substances.[192] In addition, these fluorine atoms often have a great influence on inter- and intramolecular interactions via C−F···H, F···S, and C−F···π_F interactions.[191,193] Applying fluorine substitution in the D−A polymers was investigated by You and co-workers in two recent studies.[45,61] In one report, they added two fluorine atoms to the commonly employed benzothiadiazole (BT), converting BT into fluorinated benzothiadiazole (ffBT) (Figure 18).[61] The
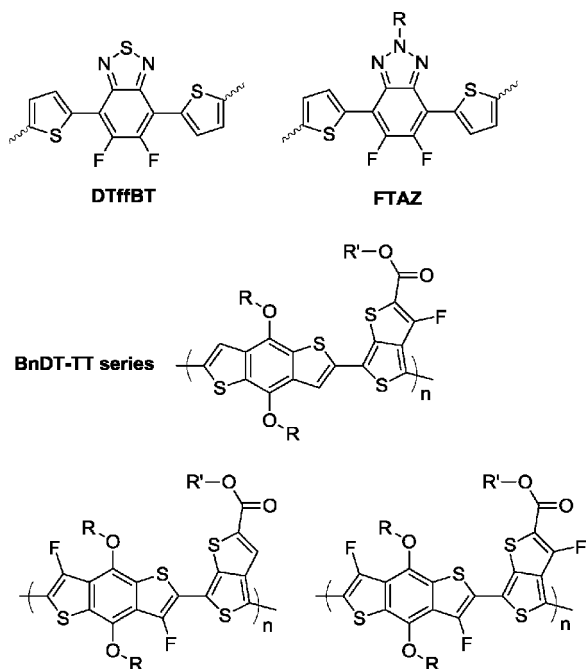
Figure 18. Chemical structures of fluorine atom containing acceptor units and conjugated polymers.

ffBT-based polymer showed decreased HOMO and LUMO levels but a similar band gap when compared with those of its nonfluorinated analogue. Preliminary PV tests on BHJ devices demonstrated both increased V_{oc} (0.91 V) and J_{sc} (12.9 mA/cm^2). Together with an also enhanced fill factor of 0.61, an impressive PCE of 7.2% was thus obtained without special treatments. In another related study, BnDT-based copolymers (PBnDT-FTAZ) with 5,6-difluoro-2H-benzo[d][1,2,3]triazole (FTAZ) as the acceptor unit was synthesized.[45] This polymer exhibited a medium band gap of 2.0 eV when compared with that of the DTBT-based polymer due to the weaker electron affinity of the FTAZ unit. Surprisingly, in spite of a band gap of ∼2.0 eV, the J_{sc} of PBnDT-FTAZ based BHJ solar cells could reach over 12 mA/cm^2 (depending upon the thickness of the active layer), which can be explained by the high molecular weight and the large hole mobility of PBnDT-FTAZ. The BHJ devices based on PBnDT-FTAZ consistently showed a higher FF and J_{sc} than those of devices based on the polymers without fluorine substituents (PBnDT-HTAZ) at comparable thicknesses. A peak PCE of 7.1% was obtained in BHJ devices of PBnDT-FTAZ:PC$_{61}$BM without annealing or any additives. Remarkably, PBnDT-FTAZ:PC$_{61}$BM solar cells can still achieve over 6% efficiency even at an unprecedented thickness of 1 μm (of the active layer).

Besides the study on the fluorine substituent effect in D−A polymers, the fluorine atom has also been applied in quinoid polymers. For example, Yu and co-workers studied a series of polymers based on fluorinated thienothiophene (TT).[74,78,194,195] As expected, the substitution of electron-withdrawing fluorine

onto the polymer backbone reduced the HOMO energy levels of polymers when compared with the nonfluorinated analogues. Furthermore, this structural modification optimized the polymers' spectral coverage of absorption and their hole mobility as well as their miscibility with PC$_{71}$BM. All these contributed to an enhanced polymer solar cell performance up to 7.4%, which is one of the highest efficiencies within the literature reports.[74,78] Further, using the original conjugated backbone (BnDT-TT) as the subject of study, Son et al. showed that the incorporation of the fluorine onto various positions of the polymer backbone significantly affected the performance of related solar cells (Figure 18).[76] Depending upon which hydrogen of the conjugated backbone is substituted by the fluorine, PCE of corresponding BHJ devices can vary from 2.3% to 7.2%. They also observed that fluorination of the BnDT unit lowered both the HOMO and LUMO levels of the conjugated polymer but widened the band gap. Finally, perfluorination of the polymer backbone led to a poor compatibility of the polymer with PC$_{71}$BM; thus, poor solar cell performance was observed. In addition, the authors found that perfluorination of the polymer backbone resulted in poor photochemical stability against singlet oxygen attack.[76] These interesting effects of substituents on physical properties of conjugated polymers are still under active investigation.

2.5. Side Chains. For conjugated polymers used in organic solar cells, solubilizing side chains are required to allow solution processability, which is the key feature for future low-cost mass production of these flexible solar cells. Without solubilizing chains, the conjugated backbone would adopt a more planar structure, thereby facilitating the chain−chain interactions among polymers and leading to unprocessable "bricks". In addition to imparting the solubility to conjugated polymers, side chains have been discovered to play important roles in certain key properties of conjugated polymers, such as molecular weight, inter- and intramolecular interactions, charge transport, and active layer morphology.[50] In this section, these recently emerged understandings of the side-chain effect will be discussed, followed by the suggested guidelines of designing solubilizing chains.

2.5.1. Position. It is well-known that decorating the polymer backbone with side chains can effectively improve the solubility of the polymer, which is a crucial prerequisite toward achieving high molecular weight of the resulting conjugated polymer. However, substituting the small hydrogen atoms on these aromatic units with rather big alkyl or alkoxy chains often result in significant steric hindrance between these aromatic units on the conjugated backbone. For example, a computational simulation revealed that severe steric hindrance introduced by these alkyl/alkoxy chains on the DTBT would lead to a twisted conjugated backbone in polymers incorporating the substituted DTBT.[196] Therefore, the hole mobilities of the polymers incorporating such substituted DTBT were noticeably lower than that of the polymer with unsubstituted DTBT, which accounted for a smaller J_{sc} in the former case.[196] In an earlier study, the homopolymers of alkylated DTBT were prepared by Jayakannan et al. by varying alkyl chains on either 3- or 4-positions of the thienyl groups.[197] Though relatively high molecular weight polymers were obtained, the steric hindrance introduced by these alkyl chains in these polymers led to much larger band gaps than that of the homopolymer of unsubstituted DTBT.[198] Later, Wang et al. synthesized a series of internal donor−acceptor type of copolymers containing benzothiadiazole (BT) and four thiophenes incorporating side

chains on different position as shown in Figure 19.[199] Despite indentical alkyl side chains, the positions where these alkyl side
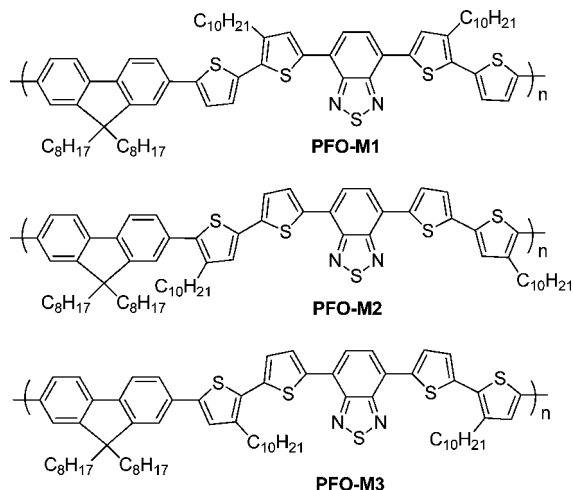
Figure 19. Chemical structures of PFO-M1, PFO-M2, and PFO-M3.

chains are attached to different thiophene rings have significant influence on the physical properties and photovoltaic performance of resulting polymers. Positioning these alkyl chains close to the fluorene renders large steric hindrance during polymerization, which results in a significantly lower molecular weight of PFO-M2 and consequently a poor PV performance of related BHJ cells when compared with 1.82% for PFO-M1 and 2.63% for PFO-M3 based BHJ solar cells.

Most recently, You and co-workers systematically investigated what effect the side-chain positions had on the optical, electrochemical, and photovoltaic properties of conjugated polymers using PBDT-DTBT as the model polymer (Figure 20).[159]
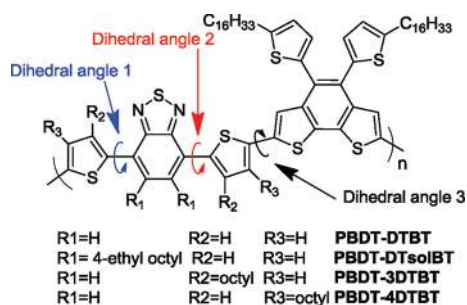
Figure 20. Chemical structures of PBDT-DTBT, PBDT-4DTBT, PBDT-3DTBT, and PBDT-DTsolBT. Reprinted with permission from ref 159. Copyright 2010 American Chemical Society.

These three polymers with alkyl chains attached on DTBT have similar molecular weights (much higher than that of PBDT-DTBT without alkyl chains on DTBT), thereby minimizing the potential complication from the influence of different molecular weights. Thus, all observed differences in properties (optical, electrochemical, and photovoltaic) can be ascribed to the difference in where these side chains were placed. They quantitatively measured the steric hindrance introduced by these alkyl chains by calculating the dihedral angles between two thienyl groups with the center BT unit as well as with the donor BDT. There is only a slight increase of the dihedral angle between the 4-substituted thienyl group and the BDT unit in PBDT-4DTBT when compared with the original PBDT-DTBT,

indicating a minimum steric hindrance introduced by the 4DTBT. Moreover, the DFT calculation showed that the electron density is delocalized in the HOMO of PBDT-4DTBT, similar to that of PBDT-DTBT. This results in an almost negligible difference between the HOMO energy level of PBDT-DTBT and that of PBDT-4DTBT. On the other hand, moving these alkyl chains away from the vicinity of BDT unit in the case of PBDT-3DTBT and PBDT-DTsolBT decreases the steric hindrance between substituted DTBT and BDT unit, recovering small numbers on the dihedral angle 3. However, greater steric hindrance is formed between the thienyl groups and the center BT unit, as shown by a dramatic numerical increase in the dihedral angles 1 and 2. This severe steric hindrance essentially breaks the conjugation at the linkages between these thienyl groups and the BT, thereby rendering large band gaps for these two polymers (2.21 eV for PBDT-3DTBT and 2.48 eV for PBDT-DTsolBT).

The thorough investigation of this library of structurally related polymers clearly indicates that attaching alkyl chains on the 4-positions of these thienyl groups (i.e., 4DTBT) only introduces minimum steric hindrance into the related D−A polymer. Therefore, PBDT-4DTBT maintains almost identical band gap and energy levels when compared with those of PBDT-DTBT. However, these additional side chains offer a high molecular weight and excellent solubility of PBDT-4DTBT, the latter leading to a more uniform mixture with $PC_{61}BM$ with better control on the film morphology. All these features of PBDT-4DTBT contribute to a noticeably enhanced efficiency (up to 2.2%) of PBDT-4DTBT-based BHJ cells, significantly higher than that of PBDT-DTBT-based devices (0.7%).

2.5.2. Shape and Length. Even when the side chains are "properly" anchored on the conjugated backbone, the length and shape of these side chains also have a noticeable (sometimes substantial) impact on the properties of resulting conjugated polymers. Gadisa et al. completed a comparative investigation on the photovoltaic properties of BHJ devices based on a series of poly(3-alkylthiophene)s of butyl (P3BT), pentyl (P3PT), and hexyl (P3HT).[200] FF of 0.529, 0.624, and 0.675 were obtained from solar cells based on P3BT:$PC_{61}BM$ (1:0.8), P3PT:$PC_{61}BM$ (1:1), and P3HT:$PC_{61}BM$ (1:1), respectively. Bipolar measurements made by field-effect transistors showed a decrease in the hole mobility and an increase in the electron mobility with increasing alkyl chain length, which is attributed to the an increase in the degree of phase separation. The longer side chains facilitate the clustering of $PC_{61}BM$ molecules and establish fast electron-percolation pathways, leading to improved electron mobility. Since holes and electrons exhibit well-balanced mobilities in the case of P3HT:$PC_{61}BM$, a better fill factor was observed.

In another study, Egbe et al. grafted different side chains to the backbone of a series of anthracene-containing poly(*p*-phenyleneethynylene)-*alt*-poly(*p*-phenylenevinylene) (PPE−PPV) copolymers to tune the π−π stacking ability of the materials (Figure 21).[201] Polymers with octyloxy substitution close to the AnE units (*ab, ad, ae*) arrange in a stacked manner, whereas asymmetric (*cc*) or branched side chain substitution (*bb, ba*) near the AnE unit yields less organized or even amorphous polymers. The best performance of 3.14% was achieved from BHJ devices based on *ab* ANE-PV which shows both stacking ability and biggest π−π stacking distance of 0.386 nm as opposed to 0.380 nm for the other polymers in this series. Lower efficiency values were obtained for the BHJ devices based on amorphous polymers *ba* and *bb*, due to a high miscibility of components in the active layer resulting in insufficient percolation paths for the
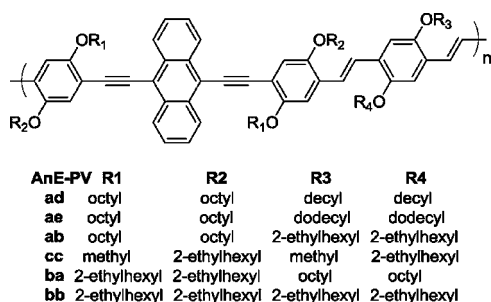
Figure 21. Chemical structures of PPE-PPV with different alkyl side chains. Reprinted with permission from ref 201. Copyright 2010 American Chemical Society.

photogenerated charges. Moreover, BHJ devices based on *ad* and *ae* with higher side chain density (number of carbons) exhibited lower photovoltages and fill factors and thus lower photovoltaic performance when compared with those of *ab* based BHJ devices. The authors believed that high density side chains dilute the concentration of the light absorbing conjugated species per volume unit and reduce the amount of light absorbed by the active layer. High density side chains also reduce the interfacial area between the DONOR polymer and the PC$_{61}$BM, leading to a strong phase separation and concomitant poor PV performance. Finally, a large V_{oc} change from ~0.65 V to ~0.90 V was observed, which is likely influenced by the shape and size of these side chains. However, the relationship between the V_{oc} and the side chains (shape and size) was not further investigated in the report.

The first quantitative analysis of the influence from the size of these side chains on photovoltaic properties of polymer–fullerene solar cells was carried out by You and co-workers.[50] In their report, six polymers with an identical polymer backbone (PNDT-DTBT) but different side chains (i.e., size and branching) were synthesized and investigated (Figure 22a). In good solvent and at high temperature, all polymer chains are completely solvated with minimum intermolecular interactions, which leads to almost identical UV–vis absorptions due to the

identical backbone of PNDT-DTBT. However, BHJ solar cells employ the polymer:PC$_{61}$BM blend at the solid state where the intermolecular interactions (i.e., between polymers and between the polymer and the PC$_{61}$BM molecules) play a crucial role. Since these seemingly subtle differences in the polymer structures (size and branching of these side chains) affect the intermolecular interactions in the solid state, the observed V_{oc} and J_{sc} of these polymer-based BHJ devices can vary as much as 100%. Consequently, the overall efficiency of these solar cells has shown a significant variation as much as 2.5-fold (from 1.20% to 3.36%). More importantly, the observed V_{oc} change was quantitatively correlated with a pre-exponential dark current term, J_{so}, which accounts for the intermolecular interactions in the polymer/PC$_{61}$BM blends. There is excellent agreement between the experimentally observed V_{oc} values and the calculated ones using the following theoretical equation (Table 7), a clear indication of the viability and effectiveness of this simulation for V_{oc}:

$$ V_{oc} \approx \frac{nkT}{q} \ln\left(\frac{J_{sc}}{J_{so}}\right) + \frac{\Delta E_{DA}}{2q} $$

where q is the fundamental charge, n is the diode ideality factor, and ΔE_{DA} is the energy difference between the LUMO level of the ACCEPTOR and the HOMO level of the DONOR.

Specifically, the polymer with the long and branched side chains (C10,6–C6,2) displayed the highest V_{oc} of 0.81 V in its BHJ cells. As the long branched chains were systematically converted to short linear chains—until the extreme of the polymer C8–C8—the measured V_{oc} gradually decreased to a minimum of 0.41 V (Table 7). From the XRD spectrum, the very weak (010) peak intensity in the C10,6–C6,2 polymer indicates a weak π-overlapping among individual conjugated polymer chains which results in weak intermolecular interaction (Figure 22b). This weak intermolecular interaction leads to a small J_{so} that is beneficial to the V_{oc} (see above equation). On the other hand, short and straight side chains would promote the
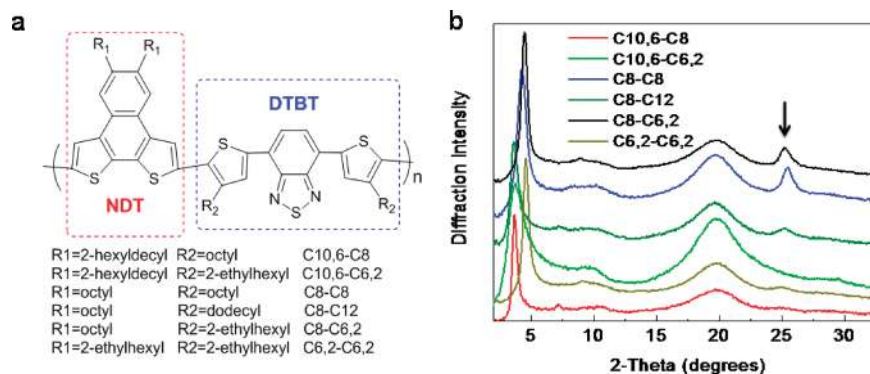
Figure 22. (a) Chemical structures of six polymers based on the PNDT-DTBT backbone. (b) XRD spectra of conjugated polymers:PC$_{61}$BM (1:1) blends in thin films (arrows indicating (010) peaks).[50]

Table 7. Measured and Calculated Performance Parameters for All Devices of PNDT-DTBT Series[50]

polymer	J_{so} (mA/cm^2)	HOMO (eV)	V_{oc} (V) cal	V_{oc} (V) exp	J_{sc} (mA/cm^2)	FF	PCE (%)
C10,6–C8	148	−5.32	0.60	0.59	7.98	0.46	2.17
C10,6–C6,2	3.38	−5.33	0.83	0.81	5.62	0.44	2.01
C8–C8	399	−5.13	0.39	0.41	6.97	0.42	1.20
C8–C12	254	−5.27	0.53	0.52	5.88	0.42	1.28
C8–C6,2	68.8	−5.30	0.60	0.59	10.93	0.46	3.00
C6,2–C6,2	22.6	−5.34	0.70	0.69	10.67	0.46	3.36

intermolecular interaction, as confirmed by the highly intense (010) peak. This improved intermolecular interaction (represented by a large J_{so}) renders a small optical band gap and better charge transport, which should increase the J_{sc} (though at the expense of V_{oc}). The short and branched side chains (C6,2–C6,2) strike a desirable balance between V_{oc} and J_{sc} to reach the optimum efficiency via an appropriate J_{so}. Therefore the C6,2-C6,2 polymer based BHJ cells exhibited the highest efficiency of 3.36% in this study with a V_{oc} of 0.69 V and a J_{sc} of 10.67 mA/cm^2.

A similar impact of these side chains has also been observed by Yu and co-workers on a series of low-band-gap polymers with identical conjugated backbone of poly(thieno[3,4-b]-thiophene−benzodithiophene) (Figure 23).[74,194,202] The first

PTB1: X=H, R1= n-dodecyl,   R2 = n-octyloxy
PTB2: X=H, R1= 2-ethylhexyl,   R2 = n-octyloxy
PTB3: X=H, R1= 2-ethylhexyl,   R2 = n-octyl
PTB4: X=F, R1= n-octyl,   R2 = 2-ethylhexyloxy
PTB5: X=H, R1= n-octyl,   R2 = 2-ethylhexyloxy
PTB6: X=H, R1= 2-butyloctyl,   R2 = n-octyloxy
PTB7: X=F, R1= 2-ethylhexyl,   R2 = 2-ethylhexyloxy
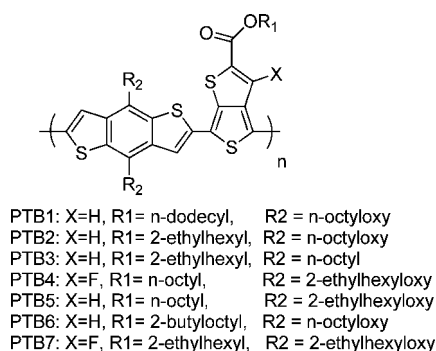
Figure 23. Chemical structures of polymers PTB1−PTB7.[202]

six polymers (PTB1 to PTB6) have similar weight-averaged molecular weights between 19.3 and 25.0 kg/mol with a relatively narrow polydispersity index (PDI) between 1.25 and 1.50, indicating that the changes in monomer structures did not lead to significant changes in the polymerization reaction. A clear relationship between properties and structure was observed from the careful study of these six polymers. Generally, the branched side chain grafted polymers (PTB2 through PTB6) show larger V_{oc} in their related BHJ devices than that of PTB1 with only straight side chains, partly due to lower HOMO energy levels of these polymers of branched side chains. However, too bulky side chains reduce the miscibility of polymer with PC$_{61}$BM, leading to excessive phase separation between polymer chains and PC$_{61}$BM molecules and thereby reducing the interfacial areas for charge separation in PTB5- or PTB6-based solar cells. The related smaller currents lead to the diminished solar cell performances in the case of PTB5 or PTB6.

To further understand the effect of side chains on the performance of solar cells based on the PTB series, both GIWAXS and GISAXS were employed to investigate the film morphology of these six polymers and their blends with PC$_{61}$BM/PC$_{71}$BM, along with PTB7 which shows an impressive efficiency as high as 7.4% of its BHJ cells.[202] Both the π−π stacking interactions in the polymer domains and PC$_{61}$BM/PC$_{71}$BM incorporation into these domains are very sensitive to the structure of the side chains attached to the TT or the BnDT subunits of the PTB polymers. The branched side chains attached on the BnDT unit cause an increase in the π−π stacking spacing in thin films and a decrease in the efficiency of related BHJ devices, while the branched side chain attached on the TT unit does not interfere with the π−π stacking spacing in the film and enhances the device efficiency. On the other hand, linear alkyl side chains occupy less space than branched alkyl

side chains, resulting in a π−π stacking distance of 3.65 Å for PTB1 vs 3.89 Å for PTB5. A striking relationship between the fill factor (FF) of related BHJ devices and the π−π stacking distances of the seven PTB polymers was also revealed, which indicates that a closer π−π stacking distance in the polymer film gives a larger FF of its corresponding BHJ device. This behavior was ascribed to the fact that the PTB polymers with the strongest π−π stacking should have the most crystalline polymer domains and bind most strongly to the anode interfacial layer, facilitating electronic communication across the interface.

The studies on PTB polymers also reveal that devices based on the fluorinated polymers (PTB4 and PTB7) show larger V_{oc} than those of other PTB polymers, mainly because the electron-withdrawing nature of these fluorine atoms leads to observed lower HOMO energy levels of PTB4 and PTB7. Moreover, the comparison of PTB2 and PTB3 discloses that replacing the octyloxy side chains with octyl side chains improves the V_{oc} of related BHJ devices from 0.6 V of PTB2 to 0.74 V in the case of PTB3. These alkoxy groups anchored on BnDT ring are strongly electron-donating, which can raise the HOMO energy level of resulting polymers and lead to the observed reduction in V_{oc}. The differences between alkyl chains and alkoxy side chains will be further discussed in the next section.

2.5.3. Alkoxy vs Alkyl. Compared with alkyl groups, alkoxy groups are more electron-donating, which usually raise up the HOMO energy level of related conjugated polymers when they are attached with alkoxy side chains. Shi et al. studied a series of poly(thiophene)s with alkoxy side chains.[203] Table 8 compares

**Table 8. Optical and Electronic Properties of P3HT, P3DOT, and POT-co-DOT**

polymer	λ_{max} (nm)		E_g^{opt} (eV)	HOMO (eV)	LUMO (eV)
	CHCl$_3$ soln	film			
P3HT	425	514	1.92	−4.75	−2.83
P3DOT	565	624	1.60	−4.47	−2.87
POT-co-DOT	538	621	1.64	−4.55	−2.91

the optical and electronic properties of regioregular P3HT, regioregular poly(3-decyloxythiophene-2,5-diyl) (P3DOT), and regioregular copolymer poly(3-octylthiophene-2,5-diyl-co-3-decyloxythiophene-2,5-diyl) (POT-co-DOT). P3DOT demonstrates an optical absorption maximum at longer wavelength than that of the P3HT. This can be attributed to both the electron-donating effect of the alkoxy group and the more coplanar backbone of the P3DOT than that of the P3HT (because of the smaller size of O than that of CH$_2$). It is not surprising that when the alkyl chains are only partially replaced by alkoxy groups in the case of POT-co-DOT, the HOMO energy level and band gap of this regioregular copolymer are in between those of P3DOT and P3HT. Similar effect of the electron-donating alkoxy group was also reported by Hou et al. on conjugated polymers with benzo-[1,2-b:3,4-b]dithiophene (BnDT) and 4,7-dithiophen-2,1,3-benzothiadiazole (DTBT) units.[204]

When the steric hindrance is not a primary concern, employing alkyl chains rather than alkoxy chains will lower the HOMO energy level of resulting polymers and increase the V_{oc} of related BHJ solar cells. This was best illustrated by the studies on PBDTTT series (structures shown in Figure 24).[74,205] The HOMO level of the original PBDTTT-E was successfully reduced by replacing the alkoxy group on the carbonyl of the
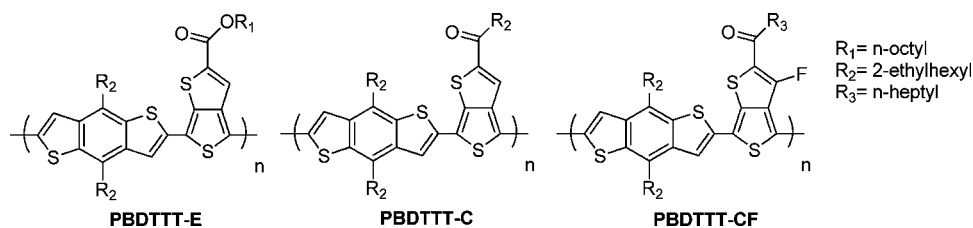
Figure 24. Chemical structures of PBDTTT-E, PBDTTT-C and PBDTTT-CF.[74] Reprinted with permission from ref 74. Copyright 2009 Nature Publishing Group.
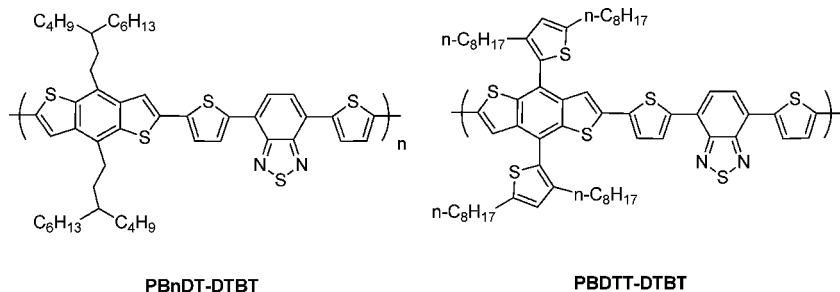
Figure 25. Chemical structures of PBnDT-DTBT and PBDTT-DTBT.
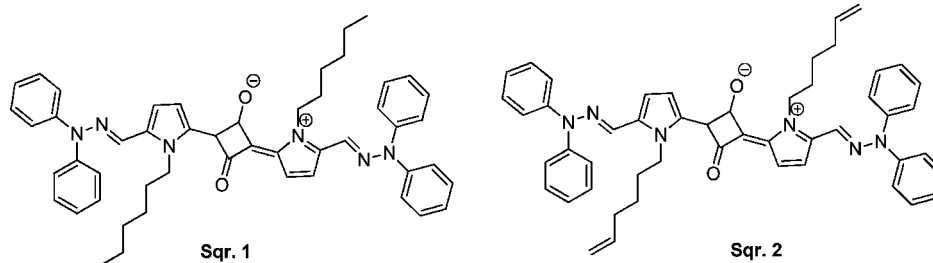
Figure 26. Chemical structures of squaraine **1** and squaraine **2**.[207]

thieno[3,4-*b*]thiophene unit with an alkyl side chain (hereafter referred to as PBDTTT-C). Because of its low HOMO level, a V_{oc} of 0.70 V was obtained in the device based on PBDTTT-C, 0.12 V higher than that of the PBDTTT-E/PC$_{71}$BM-based device. Interestingly, the substitution of the alkoxy by the alkyl group almost has no influence on the band gap for this kind of polymer, implying a complete delocalization of electronic states in low-band-gap polymers based on quinoid structures. Therefore, devices based on PBDTTT-C maintain a high J_{sc} of 14.7 mA/cm^2, with an overall PCE reaching 6.58%. Further structural modification was accomplished by substituting the hydrogen atom on the thienothiophene with a fluorine (as discussed in section 2.4), which converted the PBDTTT-C into PBDTTT-CF. As expected, the introduction of fluorine further lowered both the HOMO and LUMO levels, resulting in a similar band gap when compared with those of other PBDTTT-based polymers. Thus, the V_{oc} of devices based on PBDTTT-CF can be further increased to 0.76 V. Combined with a high J_{sc} and a fill factor (*FF*), a very impressive average PCE of 7.38% was achieved in the PBDTTT-CF-based BHJ cells.[74] The highest measured PCE is 7.73%, which is the highest efficiency value for polymer solar cells as reported in the literature.

2.5.4. Other Side Chains. Adding additional aromatic units (not fused) to the conjugated backbone as part of the side chains has also been explored. For example, Yang and co-workers incorporated additional thienylene units to the original PBnDT-DTBT (Figure 25).[6] The resulting polymer PBDTT-

DTBT-based solar cells exhibited a high V_{oc} of 0.92 V and a high J_{sc} of 10.7 mA/cm^2, which are almost 0.1 V and 3 mA/cm^2 larger than those of PBnDT-DTBT-based solar cells.[206] Consequently, the overall efficiency increased from 3.85% of PBnDT-DTBT-based devices to 5.66% of PBDTT-based ones. Interestingly, since both PBDTT-DTBT and PBnDT-DTBT exhibited similar HOMO levels and band gaps, the improved V_{oc} and J_{sc} of PBDTT-DTBT-based devices cannot be simply attributed to a lower HOMO level or a smaller band gap introduced by these thienylene groups. It is plausible that these side chains with bulky thienylene groups decrease the inter-molecular interaction between polymer and fullerene deriva-tives, leading to an enhanced V_{oc}. Also, it is likely that an improved carrier transport introduced by these thienylene groups helps increase the J_{sc}.

Lastly, Bangis et al. reported characterization of BHJ solar cells based on two new squaraine dyes, substituted at the pyrrolic nitrogen with *n*-hexyl (squaraine **1**) or *n*-hexenyl (squaraine **2**) chains (Figure 26).[207] Squaraine **2**-based devices invariably outperform those based on hexyl-substituted squaraine **1**. This performance improvement predominantly arises from the J_{sc} enhancement. To further understand the property differences between squaraine **1** and squaraine **2**, the crystal structures of these two dyes were investigated. The data reveal that the *n*-alkenyl substituent affords a more compact solid-state structure, enhancing charge mobility (thin film transistor hole mobility is increased by ~5 times) and hence increasing J_{sc}.

Although this report investigated only the side-chain effect on small molecules, it implies a new structural strategy of conjugated polymer to enhance charge transport efficiency via noncovalent alkenyl−phenyl contacts by incorporating alkenyl side chains to the polymer backbone.

3. OUTLOOK AND CHALLENGES

3.1. Maximum Efficiency Reachable with Polymer: Fullerene BHJ Solar Cell. Tremendous progress has been made in the past 16 years in the field of polymer solar cells, particularly in the design and synthesis of novel conjugated polymers as discussed in previous sections. The record high efficiency has been constantly updated in the past 3 years by the synergistic efforts between the academic researchers (e.g., design and synthesis of new polymers) and companies (e.g., device optimizations). Furthermore, the design and synthesis of these novel polymers would not have been possible without a deeper understanding of the governing physical principles,[33,208,209] device physics,[31,51,210] and morphology investigation and control.[211−216] As a result of the synergy in the community (including both academia and companies), the J_{sc} can reach as high as 17.3 mA/cm²,[5,217] the highest V_{oc} obtained has been over 1 V,[41−43] and the highest obtained FF has breached 70%.[44,45] If we could achieve all these impressive values with one system, this champion BHJ solar cell would offer an unprecedented value of 12%! This is the bright future of the exciting field of polymer solar cells and also the goal that numerous researchers strive for. Unfortunately, all these high values are obtained from different polymer-based BHJ systems, partly due to an intrinsic "tug of war" between J_{sc} and V_{oc}, as elaborated on in section 1.3[59] and experimentally demonstrated.[46] A more rigorous model calculation on the ultimate performance of polymer:fullerene BHJ cells was recently accomplished by Blom and co-workers (ref 218 and references therein). They predicted a maximum power efficiency of 11.7% for single junction cells and 14.1% for tandem structures. This is very encouraging, and the community is steadily approaching these numbers: for example, a new record high efficiency of 9.2% for organic solar cells has been recently reported.[9]

3.2. Even Higher Efficiency Possible? However, if polymer solar cells (and organic solar cells in general) intend to compete with other thin film PV technologies (such as CIGS or CdTe) as a viable economic solution for renewable energy future, higher efficiencies (15−20%) will be strongly desirable if not required. For example, flexible thin film solar cells based on copper indium gallium (di)selenide (CIGS) can reach an energy conversion efficiency as high as 18.7%,[219] and the efficiency of mass-produced CIGS thin film modules has breached 13%.[220] Can polymer (organic) solar cells achieve similar performances? To answer this challenge, one has to analyze the J_{sc}, V_{oc}, and FF individually, since these three parameters ultimately decide the efficiency of any solar cells. To facilitate the discussion and related recommendations, we collected roughly 200 data sets from different polymer/fullerene BHJ systems in the literature reports and plotted the J_{sc} versus the band gap of the polymer (Figure 27) and V_{oc} versus the HOMO energy level of the polymer (Figure 28). To make the analysis meaningful, we averaged all the experimental values in related intervals in both figures.

● J_{sc}: Figure 27 clearly shows that a smaller band gap favors a higher short-circuit current. However, this trend reaches its maximum around 1.3 eV. Polymers with even smaller band gap than 1.3 eV fail to offer more current as expected from their absorption extending into the near-IR. Two possible reasons
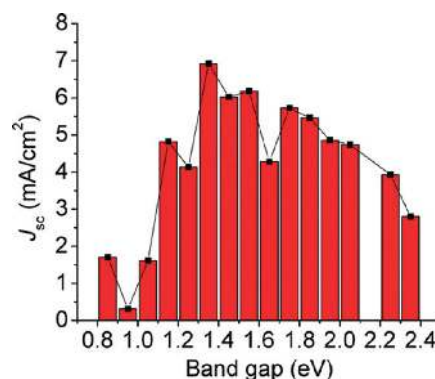
Figure 27. E_g vs J_{sc} plot. A total of ~200 data points were taken and summarized with 0.1 eV interval, e.g., 0.80−0.89, 0.90−0.99 eV.

account for this observation. The first is related with the energy levels of these polymers having extremely small band gaps. Often a very strong acceptor (such as benzobisthiadiazole) was paired with a strong donor to achieve the small band gap via the donor−acceptor low-band-gap approach; however, these strong acceptors could lower the LUMO level below −3.9 eV, leading to an inefficient exciton dissociation when $PC_{61}BM$ was used as the electron ACCEPTOR in the BHJ solar cells. The second is the usually small full width at half-maximum (FWHM) of these conjugated polymers, normally on the order of 200 nm. Thus, continuously shifting the absorption of the polymer toward the IR end of the solar spectrum would inevitably diminish its ability to absorb the light in the visible region. In addition, these near-IR/IR absorbing polymers usually have low absorption coefficients, which exacerbate the light harvesting. On the basis of these analyses, we identify a few potential directions worth of further research:

a. Choosing appropriate structural units in D−A polymers: In order to achieve a narrow band gap, a strong electron-accepting structural unit is required in donor−acceptor copolymers. However, one should develop appropriate "strong" acceptors such that they would bring the LUMO level close to but not lower than the ideal LUMO level (Figure 5). As discussed in section 2.3.2 which is focused on the design of acceptors, the relative easier approach is to fine-tune existing acceptors by attaching substituents (e.g., changing DTBT to DTffBT[61]) or changing specific atoms (e.g., switching DTBT to DTPyT[107]). A better approach—though more challenging—is to envision new designs of chemical structures. For example, one can certainly benefit from a close look at dyes and pigments since a number of of the recently developed "strong" acceptors were adapted from existing dyes. Equally important in achieving a narrow band gap is the fine-tuning of HOMO levels of these electron-donating structural units, which certainly require deliberation. As indicated in section 2.3.1 which is dedicated to the design of donors, polyaromatic units with fused aromatic rings offer noticeable advantages as donor moieties. The rigid and planar structures of these fused aromatics usually lead to strong π-interactions, which help improve the hole mobility and decrease the band gap of related conjugated polymers in the solid state. However, appropriate side chains need to be carefully selected to maintain the beneficial polymer−polymer interactions and polymer−PCBM interactions, while still providing enough solubility to the polymer (for high molecular weight and easy processability).

b. Increasing FWHM: Two possible solutions have emerged to increase the FWHM, both of which used random copolymerization to bring more than two monomers into the

conjugated backbone, though in a slightly different manner. Liang et al. incorporated the pre-quinoid unit of thieno[3,4-*b*]-thiophene (TT) into the polythiophene backbone, basically introducing the low-band-gap character of the TT into the backbone.[72] Depending upon the feed ratio of the TT vs thiophene, the band gap and the energy level of the random copolymer can be tuned. In an earlier report, Li and co-workers added another conjugated oligomer (bithienylenevinylene) to the 3-position of the thiophene and polymerized this modified thiophene unit with 3-hexylthiophene and unsubstituted thiophene monomers in a random manner into the biTV-PT.[221] These conjugated side chains add strong absorption from 350 to 480 nm, thereby leading to a broad absorption spectrum from 350 to 650 nm of these copolymers. Both reports did obtain better performance from these random copolymers than that of the benchmark P3HT in their studies, though the obtained efficiency numbers are still noticeably lower than that of the optimized P3HT-based cell (∼5%). Nevertheless, considering the effective broadening of the absorption by these approaches, further investigation is still warranted.

c. Making n-type material absorb: Alternatively, one can employ electron-accepting materials that absorb the complementary part of the solar spectrum in regard to the absorption of the electron-donating polymers, thereby broadening the light harvesting of the active layer. The most successful example is the $PC_{71}BM$, whose lesser symmetry (compared with $PC_{61}BM$) renders a much enhanced absorption from 300 to 600 nm.[15] This strong absorption in the UV−vis region by the $PC_{71}BM$ effectively complements the main absorption in the visible to NIR region by these narrow-band-gap polymers (600 to 900 nm), offered by these narrow-band-gap polymers, thereby leading to an appreciable increase (20% or more) in the J_{sc} of related solar cells when compared with that of $PC_{61}BM$-based ones. Almost all reported polymer/PCBM-based solar cells with over 7% efficiency have used $PC_{71}BM$,[60,62,74,78] with only few exceptions.[45,61] A more elegant solution comes from the design and synthesis of electron-accepting polymers with tunable absorption. Though these polymer:polymer solar cells have not reached high efficiency (highest around 2.5%[222]) as polymer:fullerene solar cells, the full tunability (e.g., energy level and band gap) of these electron-accepting polymers offers a viable approach toward not only a higher J_{sc} but also a high V_{oc} in these all polymer solar cells.

d. Improving EQE: In contrast to the internal quantum efficiency (IQE) which already reached 100% in some recent reports,[4] the external quantum efficiency (EQE) remains relatively low (50%−80%), even in these highly efficient polymers/fullerene BHJ solar cells. For example, the highest reported J_{sc} of 17.3 mA/cm^2 could have been 30 mA/cm^2 based on its band gap of 1.3 eV, if the EQE were 100% instead of the observed ∼55%.[5] This is mainly due to the low mobility of charge carriers in these polymer:fullerene blends and the intrinsically disordered morphology of the BHJ cells, which limits the optimal film thickness of the active layer to less than 200 nm. A thicker film would be able to harvest all the light within the film absorption; however, the generated charges after dissociating these excitons would not be able to transverse the thick film and reach the individual electrode before various recombination mechanisms kick in to annihilate these energy carrying charges. Thus further improving the carrier mobilities (both holes and electrons), controlling the morphology, and finding methods to slow down or even eliminate charge recombination should be among research priorities.
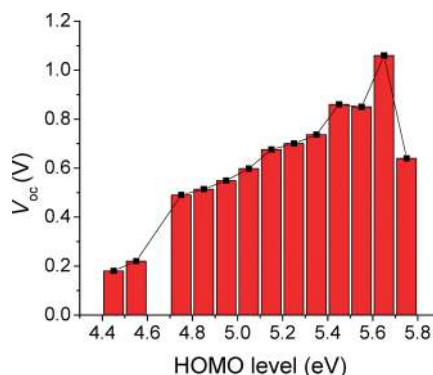
Figure 28. HOMO vs V_{oc} plot. A total of ∼200 data points were taken and summarized with 0.1 eV interval, e.g., 4.40−4.49, 4.50−4.59 eV. Please note that all HOMO energy levels should be negative. In the Y axis, the "−" sign was omitted for clarity.

• V_{oc}: A similar trend has been observed for V_{oc} vs HOMO level (Figure 28). The open-circuit voltage increases as the HOMO energy level lowers, reaching the maximum of 1.02 V around a HOMO level of −5.56 eV, and then drops.[102] This observation is not surprising since after years of investigation, it is generally accepted that the V_{oc} is proportional to the difference between the HOMO of the DONOR and the LUMO of the ACCEPTOR, though recent advances in understanding the origin of the V_{oc} have provided further insights.[48−50,223] Thus, a lower HOMO energy level (but not too low) is desirable. As shown in earlier discussion (e.g., section 2.3.1), polyaromatic units with flanking thiophene units are good candidates of such "weak" donors to offer appropriate HOMO levels in D−A conjugated polymers. This is because the electron-donating ability of those units can be fine-tuned by varying fused aromatic units and/or attaching substituents. Moreover, thiophene units are less likely to have steric hindrance with adjacent units than benzene would have. Therefore, having thiophenes as the finish for these polyaromatic units can lead to a more planar backbone with better conjugation. But is achieving a V_{oc} of 1.1 V indeed applaudable? If we took −4.2 eV as the LUMO of the $PC_{61}BM$, we would still have lost 0.4 eV from the energy difference ($E_{LUMO(ACCEPTOR)}$ − $E_{HOMO(DONOR)}$) which was not converted to the V_{oc}. This loss of 0.4 eV or more is typically observed in polymer solar cells. If we consider another source of the voltage loss, the empirical 0.3 eV between the LUMOs of the DONOR polymer and the fullerene, we have lost ∼0.7 eV altogether, which could have doubled the V_{oc} if all contributed to the V_{oc}! Therefore, much more work needs to be done on two possible fronts:

a. Further understanding the origin of V_{oc} and searching for new acceptors: First, is the empirical 0.3 eV required for effective exciton splitting at the interface really necessary? With a recently developed new π-electron ACCEPTOR (D99'BF),[224] Heeger and Wudl showed that a V_{oc} of 1.2 V could be obtained from the P3HT/D99'BF BHJ solar cell,[225] as opposed to the usually obtained 0.6 V in the case of P3HT/$PC_{61}BM$ solar cells. More importantly, these authors demonstrated that electron transfer could still occur even with only 0.12 eV in the LUMOs offset. Apparently, the exciton binding energy could be as small as 0.1 eV (at least in the case of P3HT). This exciting discovery points to a potential further increase on the V_{oc} via designing non-fullerene-based acceptors. However, even in this successful demonstration, a loss of over 0.5 eV was still observed since the difference between the LUMO of D99'BF and the HOMO of

P3HT was 1.78 eV. This leads to the second question: can we minimize the commonly observed loss of 0.4–0.6 eV from the energy level difference between $E_{LUMO(ACCEPTOR)}$ and $E_{HOMO(DONOR)}$? There have been some suggestions that reducing the electron–phonon coupling of these excitons thereby smaller Stokes shift would help diminish this loss mechanism.[226] This would call for well-ordered polymers with delocalized excitons. Further, recent advances in further understanding of the V_{oc} suggest that reducing the electronic coupling between the polymer and the fullerene would increase the V_{oc}.[48−50,223] Nevertheless, there is still a lot to be done to determine a clearer structure–property relationship regarding the V_{oc}, so the synthetic chemists will know how to design better materials (both electron-donating and electron-accepting materials).

b. Engineering the fullerene: Alternatively, before we find new acceptors that can replace the fullerene on all fronts, we can still modify the structure of this fascinating group of molecules to raise up their LUMO energy levels in order to gain a higher V_{oc}. There have been successful examples such as trimetallic nitride endohedral fullerenes (TNEFs, in particular $Lu_3N@C80$),[13] indene-C_{60} bisadduct (ICBA),[16] among others.[227] The V_{oc} of related P3HT:modified fullerene BHJ cells can be increased as much as 0.26 V[16] when compared with P3HT/$PC_{61}BM$ cells because of the raised LUMO energy level of the modified fullerene.

● *FF*: Unlike silicon solar cell or even dye-sensitized solar cells, both of which give high fill factors (75%−80% or higher), the polymer solar cells usually only offer a fill factor around 60%. The fill factor is ultimately determined by the series resistance (R_s) and the shunt resistance (R_{sh}) of the devices. Because of the low charge carrier mobilities (especially holes) and the disorded nature of the BHJ film, BHJ solar cells usually have a relatively high R_s and relatively low R_{sh}. In order to get a high FF, one would require to achieve both a low R_s and a high R_{sh}. Research efforts are needed to reach a balanced and rapid charge transport (holes vs electrons), to optimize and control the film morphology into more ordered structure, and to improve all electric contacts.

● *Morphology*: The full potential of any conjugated polymer for solar cells can only be realized with an optimized morphology. Though there is a general consensus regarding what defines a preferred morphology (i.e., interpenetrating network at nanometer scale), the "ideal" morphology could vary from one polymer/fullerene system to the other. How to control the morphology poses an even bigger challenge, though considerable progress has been made,[228] particularly the annealing (via thermal or solvent) and the discovery of processing additives.[211,213,216] The interactions between DONOR polymers, between DONOR polymer and fullerene ACCEPTORS and between fullerene ACCEPTORS all contribute to the formation of the morphology in a thin film. First, the interaction between DONOR polymers is dominated by the π−π interaction among conjugated backbones, which can bring polymer backbones close enough to form stacked polymer clusters. This stacking is beneficial for charge transport between polymer chains. However, too strong π−π interactions can lead to the formation of large polymer-rich domains, resulting in a low hole mobility across the entire film due to multiple crosses over grain boundaries. In addition to the conjugated backbone, the side chains can also impact the intermolecular interaction as discussed in section 2.5. Therefore, both conjugated backbone and side chains need to be carefully designed in order to control the polymer−polymer interaction such that these polymers can form desired "channels" to facilitate the charge transport. Second, the polymer−fullerene interactions and their contribution to the morphology are even more complicated. Progress has been made, though. For example, McGehee and co-workers showed that fullerene derivatives were intercalated between the polymer side chains in some polymer:fullerene blends.[147,148,229] This intercalation is important in determining the optimal polymer:fullerene ratio. For example, in blends where intercalation occurs, fullerenes must fill all available space between the polymer side chains prior to the formation of a pure electron-transporting fullerene phase. This intercalation would also affect some important device characteristics such as mobility, light absorption, photoluminescence, and recombination due to the intimate mixing of the polymer DONORS and fullerene ACCEPTORS in the intercalated phase. In short, we are still in the early stage of fully understanding the morphology of polymer:fullerene blends in thin films. Further development of analytical tools to unveil the "true" morphology of highly efficient BHJ systems, and novel approaches to render the ideal morphology (via chemical design or physical methods), should remain on the top of research priorities.

3.3. Other Pertinent Issues. Though the constitution of the active layer (i.e., polymer and fullerene or other ACCEPTORS) ultimately determine the maximum efficiency achievable with the BHJ cell, one still needs to solve a number of other issues before reaching the full potential of any given cell. Listed below are a few other active research fronts:

● *Interfaces*: The interface between organic active layers and these two contact electrodes (cathode and anode) needs to be optimized to facilitate the charge collection and minimize any loss.[230,231] Metal oxides recently emerged as versatile interface modifiers, such as NiO,[232] MoO_3,[233−235] and WO_3[236,237] as the hole transport layer and TiO_x[37,238] and ZnO[239−242] as the electron transport layer.

● *Device engineering*: Progress has been made in the inverted cells (to increase the air stability),[243] applying light trapping for better light harvesting,[244] and using tandem structure[245] to increase the overall efficiency of polymer solar cells.

In addition, to achieve the commercial viability, the community still needs to work on the following issues:

● *Transparent contact electrode (TCO)*: ITO has been the standard TCO for polymer solar cells. However, the physical nature (brittleness) and the high price associated with ITO prevent a large-scale production of polymer solar cells based on this particular material. Carbon nanotubes, graphenes,[246−254] and metal nanowires[255,256] have been proposed, and respectable results have been obtained.

● *Stability*: Significant progress has been made; for example, Konarka has shown a lifetime of 3 years for their polymer solar cells.[257]

All these challenges (also opportunities) compose the major part of the rather long wish list for the research community of polymer (organic) solar cells. This is a tall order; however, if we could achieve these goals via collaborative efforts, the payoff would be huge—single junction polymer solar cells with 15% efficiency would be within reach (for example, a band gap of 1.3 eV with an EQE of 80%, a V_{oc} of 0.8 V, and a FF of 0.75)!

■ AUTHOR INFORMATION

Corresponding Author
*E-mail: wyou@unc.edu.

BIOGRAPHIES

Huaxing Zhou obtained his B.S. degree in polymer chemistry from the University of Science and Technology of China in 2007. He recently received his Ph.D. degree from the department of Chemistry at the University of North Carolina at Chapel Hill under the direction of Prof. Wei You (2011). His Ph.D. research was focused on the rational design of conjugated polymers for organic solar cells. He is currently a postdoctoral fellow in the research group of Prof. Jeremiah A. Johnson at Massachusetts Institute of Technology.
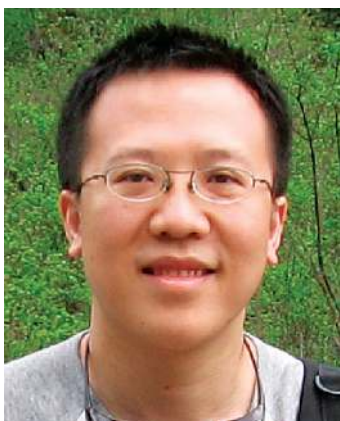
Liqiang Yang is currently a PhD candidate under the guidance of Prof. Wei You at the University of North Carolina at Chapel Hill. He received his B.S. degree in material sciences and engineering at Xi'an Jiaotong University in 2004 and obtained an M.S. degree in material engineering at the University of Wisconsin–Milwaukee in 2007. His current research focus is the fundamental understanding the structure–properties relationships of novel polymers for organic solar cells.

Wei You was born in a small village outside of Chuzhou in Anhui Province of China and grew up in Hefei, the provincial capital of Anhui. After receiving a B.S. degree in Polymer Chemistry from University of Science and Technology of China in 1999, he attended the graduate program of chemistry at the University of Chicago, where he obtained his Ph.D. in 2004 under the guidance of Professor Luping Yu. He then moved west and finished his postdoctoral training at Stanford University in 2006 with Professor Zhenan Bao. In July 2006, he joined the University of North Carolina at Chapel Hill as an Assistant Professor in Chemistry. Professor You's research interests focus on the development of novel multifunctional materials for a variety of applications, including organic solar cells, molecular electronics, and spintronics.

REFERENCES

(1) Bijleveld, J. C.; Zoombelt, A. P.; Mathijssen, S. G. J.; Wienk, M. M.; Turbiez, M.; de Leeuw, D. M.; Janssen, R. A. J. *J. Am. Chem. Soc.* **2009**, *131* (46), 16616−16617.

(2) Lewis, N. S. *Science (Washington, DC, U. S.)* **2007**, *315* (5813), 798−801.

(3) Yu, G.; Gao, J.; Hummelen, J. C.; Wudl, F.; Heeger, A. J. *Science (Washington, DC, U. S.)* **1995**, *270* (5243), 1789−1791.

(4) Park, S. H.; Roy, A.; Beaupre, S.; Cho, S.; Coates, N.; Moon, J. S.; Moses, D.; Leclerc, M.; Lee, K.; Heeger, A. J. *Nature Photonics* **2009**, *3* (5), 297−302.

(5) Coffin, R. C.; Peet, J.; Rogers, J.; Bazan, G. C. *Nature Chem.* **2009**, *1* (8), 657−661.

(6) Huo, L.; Hou, J.; Zhang, S.; Chen, H.-Y.; Yang, Y. *Angew. Chem., Int. Ed.* **2010**, *49* (8), 1500−1503.

(7) Xiao, S.; Price, S. C.; Zhou, H.; You, W. *ACS Symp. Ser.* **2010**, *1034*, 71−80.

(8) Kirchmeyer, S.; Reuter, K. *J. Mater. Chem.* **2005**, *15* (21), 2077−2088.

(9) Service, R. F. *Science (Washington, DC, U. S.)* **2011**, *332* (6027), 293.

(10) Cheng, Y.-J.; Yang, S.-H.; Hsu, C.-S. *Chem. Rev. (Washington, DC, U. S.)* **2009**, *109* (11), 5868−5923.

(11) Chen, J.; Cao, Y. *Acc. Chem. Res.* **2009**, *42* (11), 1709−1718.

(12) Facchetti, A. *Chem. Mater.* **2010**, *23* (3), 733−758.

(13) Ross, R. B.; Cardona, C. M.; Guldi, D. M.; Sankaranarayanan, S. G.; Reese, M. O.; Kopidakis, N.; Peet, J.; Walker, B.; Bazan, G. C.; Van Keuren, E.; Holloway, B. C.; Drees, M. *Nature Mater.* **2009**, *8* (3), 208−212.

(14) Lenes, M.; Wetzelaer, G.-J. A. H.; Kooistra, F. B.; Veenstra, S. C.; Hummelen, J. C.; Blom, P. W. M. *Adv. Mater.* **2008**, *20* (11), 2116−2119.

(15) Wienk, M. M.; Kroon, J. M.; Verhees, W. J. H.; Knol, J.; Hummelen, J. C.; van Hal, P. A.; Janssen, R. A. J. *Angew. Chem., Int. Ed.* **2003**, *42* (29), 3371−3375.

(16) He, Y.; Chen, H.-Y.; Hou, J.; Li, Y. *J. Am. Chem. Soc.* **2010**, *132* (4), 1377−1382.

(17) Zhao, G.; He, Y.; Li, Y. *Adv. Mater.* **2010**, *22* (39), 4355−4358.

(18) Matsuo, Y.; Sato, Y.; Niinomi, T.; Soga, I.; Tanaka, H.; Nakamura, E. *J. Am. Chem. Soc.* **2009**, *131* (44), 16048−16050.

(19) Sariciftci, N. S.; Smilowitz, L.; Heeger, A. J.; Wudl, F. *Science (Washington, DC, U. S.)* **1992**, *258* (5087), 1474−1476.

(20) Murata, M.; Morinaka, Y.; Murata, Y.; Yoshikawa, O.; Sagawa, T.; Yoshikawa, S. *Chem. Commun. (Cambridge, U. K.)* **2011**, *47* (26), 7335−7337.

(21) Thompson, B. C.; Fréchet, J. M. J. *Angew. Chem., Int. Ed.* **2008**, *47* (1), 58−77.

(22) Kroon, R.; Lenes, M.; Hummelen, J. C.; Blom, P. W. M.; de Boer, B. *Polym. Rev. (Philadelphia, PA, U. S.)* **2008**, *48* (3), 531−582.

(23) Kippelen, B.; Bredas, J.-L. *Energy Environ. Sci.* **2009**, *2* (3), 251−261.

(24) Helgesen, M.; Sondergaard, R.; Krebs, F. C. *J. Mater. Chem.* **2010**, *20* (1), 36−60.

(25) Delgado, J. L.; Bouit, P.-A.; Filippone, S.; Herranz, M. A.; Martin, N. *Chem. Commun. (Cambridge, U. K.)* **2010**, *46* (27), 4853−4865.

(26) Heeger, A. J. *Chem. Soc. Rev.* **2010**, *39* (7), 2354−2371.

(27) Dennler, G.; Scharber, M. C.; Brabec, C. J. *Adv. Mater.* **2009**, *21* (13), 1323−1338.

(28) Günes, S.; Neugebauer, H.; Sariciftci, N. S. *Chem. Rev. (Washington, DC, U. S.)* **2007**, *107* (4), 1324−1338.

(29) Hains, A. W.; Liang, Z.; Woodhouse, M. A.; Gregg, B. A. *Chem. Rev. (Washington, DC, U. S.)* **2010**, *110* (11), 6689−6735.

(30) Po, R.; Maggini, M.; Camaioni, N. *J. Phys. Chem. C* **2009**, *114* (2), 695−706.

(31) Blom, P. W.; Mihailetchi, V. D.; Koster, L. J. A.; Markov, D. E. *Adv. Mater.* **2007**, *19* (12), 1551−1566.

(32) Krebs, F. C.; Tromholt, T.; Jorgensen, M. *Nanoscale* **2010**, *2* (6), 873−886.

(33) Brédas, J.-L.; Norton, J. E.; Cornil, J.; Coropceanu, V. *Acc. Chem. Res.* **2009**, *42* (11), 1691−1699.

(34) Shaheen, S. E.; Brabec, C. J.; Sariciftci, N. S.; Padinger, F.; Fromherz, T.; Hummelen, J. C. *Appl. Phys. Lett.* **2001**, *78* (6), 841−843.

(35) Brabec, C. J.; Shaheen, S. E.; Winder, C.; Sariciftci, N. S.; Denk, P. *Appl. Phys. Lett.* **2002**, *80* (7), 1288−1290.

(36) Reyes-Reyes, M.; Kim, K.; Carroll, D. L. *Appl. Phys. Lett.* **2005**, *87* (8), 3−6.

(37) Kim, J. Y.; Kim, S. H.; Lee, H. H.; Lee, K.; Ma, W. L.; Gong, X.; Heeger, A. J. *Adv. Mater.* **2006**, *18* (5), 572−576.

(38) Ma, W. L.; Yang, C. Y.; Gong, X.; Lee, K.; Heeger, A. J. *Adv. Funct. Mater.* **2005**, *15* (10), 1617−1622.

(39) Li, G.; Shrotriya, V.; Huang, J. S.; Yao, Y.; Moriarty, T.; Emery, K.; Yang, Y. *Nature Mater.* **2005**, *4* (11), 864−868.

(40) Kim, Y.; Cook, S.; Tuladhar, S. M.; Choulis, S. A.; Nelson, J.; Durrant, J. R.; Bradley, D. D. C.; Giles, M.; McCulloch, I.; Ha, C.-S.; Ree, M. *Nature Mater.* **2006**, *5* (3), 197−203.

(41) Gadisa, A.; Mammo, W.; Andersson, L. M.; Admassie, S.; Zhang, F.; Andersson, M. R.; Inganäs, O. *Adv. Funct. Mater.* **2007**, *17* (18), 3836−3842.

(42) Zhang, F.; Jespersen, K. G.; Björström, C.; Svensson, M.; Andersson, M. R.; Sundström, V.; Magnusson, K.; Moons, E.; Yartsev, A.; Inganäs, O. *Adv. Funct. Mater.* **2006**, *16* (5), 667−674.

(43) Zheng, Q.; Jung, B. J.; Sun, J.; Katz, H. E. *J. Am. Chem. Soc.* **2010**, *132* (15), 5394−5404.

(44) Zoombelt, A. P.; Mathijssen, S. G. J.; Turbiez, M. G. R.; Wienk, M. M.; Janssen, R. A. J. *J. Mater. Chem.* **2010**, *20* (11), 2240−2246.

(45) Price, S. C.; Stuart, A. C.; Yang, L.; Zhou, H.; You, W. *J. Am. Chem. Soc.* **2011**, *133* (12), 4625−4631.

(46) Zhou, H.; Yang, L.; Liu, S.; You, W. *Macromolecules* **2010**, *43* (24), 10390−10396.

(47) Scharber, M. C.; Mühlbacher, D.; Koppe, M.; Denk, P.; Waldauf, C.; Heeger, A. J.; Brabec, C. J. *Adv. Mater.* **2006**, *18* (6), 789−794.

(48) Perez, M. D.; Borek, C.; Forrest, S. R.; Thompson, M. E. *J. Am. Chem. Soc.* **2009**, *131* (26), 9281−9286.

(49) Vandewal, K.; Tvingstedt, K.; Gadisa, A.; Inganas, O.; Manca, J. V. *Nature Mater.* **2009**, *8* (11), 904−909.

(50) Yang, L.; Zhou, H.; You, W. *J. Phys. Chem. C* **2010**, *114* (39), 16793−16800.

(51) Moliton, A.; Nunzi, J.-M. *Polym. Int.* **2006**, *55* (6), 583−600.

(52) http://www.pveducation.org/pvcdrom/.

(53) Mauer, R.; Kastler, M.; Laquai, F. *Adv. Funct. Mater.* **2010**, *20* (13), 2085−2092.

(54) Kim, Y.; Nelson, J.; Durrant, J. R.; Bradley, D. D. C.; Heo, K.; Park, J.; Kim, H.; McCulloch, I.; Heeney, M.; Ree, M.; Ha, C.-S. *Soft Matter* **2007**, *3* (1), 117−121.

(55) Roncali, J. *Chem. Rev. (Washington, DC, U. S.)* **1997**, *97* (1), 173−205.

(56) Havinga, E. E.; ten Hoeve, W.; Wynberg, H. *Synth. Met.* **1993**, *55* (1), 299−306.

(57) Ajayaghosh, A. *Chem. Soc. Rev.* **2003**, *32* (4), 181−191.

(58) Zhang, Q. T.; Tour, J. M. *J. Am. Chem. Soc.* **1998**, *120* (22), 5355−5362.

(59) Zhou, H.; Yang, L.; Stoneking, S.; You, W. *ACS Appl. Mater. Interfaces* **2010**, *2* (5), 1377−1383.

(60) Chu, T.-Y.; Lu, J.; Beaupré, S.; Zhang, Y.; Pouliot, J.-R. m.; Wakim, S.; Zhou, J.; Leclerc, M.; Li, Z.; Ding, J.; Tao, Y. *J. Am. Chem. Soc.* **2011**, *133* (12), 4250−4253.

(61) Zhou, H.; Yang, L.; Stuart, A. C.; Price, S. C.; Liu, S.; You, W. *Angew. Chem., Int. Ed.* **2011**, *50* (13), 2995−2998.

(62) Amb, C. M.; Chen, S.; Graham, K. R.; Subbiah, J.; Small, C. E.; So, F.; Reynolds, J. R. *J. Am. Chem. Soc.* **2011**, *133* (26), 10062−10065.

(63) Su, M.-S.; Kuo, C.-Y.; Yuan, M.-C.; Jeng, U. S.; Su, C.-J.; Wei, K.-H. *Adv. Mater.* **2011**, *23* (29), 3315−3319.

(64) Wudl, F.; Kobayashi, M.; Heeger, A. J. *J. Org. Chem.* **1984**, *49* (18), 3382−3384.

(65) Pomerantz, M.; Chalonergill, B.; Harding, L. O.; Tseng, J. J.; Pomerantz, W. J. *J. Chem. Soc., Chem. Commun.* **1992**, *22*, 1672−1673.

(66) Hong, S. Y.; Marynick, D. S. *Macromolecules* **1992**, *25* (18), 4652−4657.

(67) Sotzing, G. A.; Lee, K. H. *Macromolecules* **2002**, *35* (19), 7281−7286.

(68) Qin, Y.; Kim, J. Y.; Frisbie, C. D.; Hillmyer, M. A. *Macromolecules* **2008**, *41* (15), 5563−5570.

(69) Hou, J. H.; Park, M. H.; Zhang, S. Q.; Yao, Y.; Chen, L. M.; Li, J. H.; Yang, Y. *Macromolecules* **2008**, *41* (16), 6012−6018.

(70) Wienk, M. M.; Turbiez, M. G. R.; Struijk, M. P.; Fonrodona, M.; Janssen, R. A. J. *Appl. Phys. Lett.* **2006**, *88* (15), 153511−153513.

(71) Zhang, F.; Mammo, W.; Andersson, L. M.; Admassie, S.; Andersson, M. R.; Inganäs, O. *Adv. Mater.* **2006**, *18* (16), 2169−2173.

(72) Liang, Y. Y.; Xiao, S. Q.; Feng, D. Q.; Yu, L. P. *J. Phys. Chem. C* **2008**, *112* (21), 7866−7871.

(73) Kleinhenz, N.; Yang, L.; Zhou, H.; Price, S. C.; You, W. *Macromolecules* **2011**, *44* (4), 872−877.

(74) Chen, H.-Y.; Hou, J.; Zhang, S.; Liang, Y.; Yang, G.; Yang, Y.; Yu, L.; Wu, Y.; Li, G. *Nature Photonics* **2009**, *3* (11), 649−653.

(75) Huang, Y.; Hou, L.; Zhang, S.; Guo, X.; Han, C. C.; Li, Y.; Hou, J. *Chem. Commun. (Cambridge, U. K.)* **2011**, *47* (31), 8904−8906.

(76) Son, H. J.; Wang, W.; Xu, T.; Liang, Y.; Wu, Y.; Li, G.; Yu, L. *J. Am. Chem. Soc.* **2011**, *133* (6), 1885−1894.

(77) He, F.; Wang, W.; Chen, W.; Xu, T.; Darling, S. B.; Strzalka, J.; Liu, Y.; Yu, L. *J. Am. Chem. Soc.* **2011**, *133* (10), 3284−3287.

(78) Liang, Y.; Xu, Z.; Xia, J.; Tsai, S.-T.; Wu, Y.; Li, G.; Ray, C.; Yu, L. *Adv. Mater.* **2010**, *22* (20), E135−E138.

(79) Li, Y.; Zou, Y. *Adv. Mater.* **2008**, *20* (15), 2952−2958.

(80) Huang, F.; Chen, K.-S.; Yip, H.-L.; Hau, S. K.; Acton, O.; Zhang, Y.; Luo, J.; Jen, A. K. Y. *J. Am. Chem. Soc.* **2009**, *131* (39), 13886−13887.

(81) Duan, C.; Chen, K.-S.; Huang, F.; Yip, H.-L.; Liu, S.; Zhang, J.; Jen, A. K. Y.; Cao, Y. *Chem. Mater.* **2010**, *22* (23), 6444−6452.

(82) Cravino, A.; Sariciftci, N. S. *J. Mater. Chem.* **2002**, *12* (7), 1931−1943.

(83) Giacalone, F.; Martín, N. *Chem. Rev. (Washington, DC, U. S.)* **2006**, *106* (12), 5136−5190.

(84) Ramos, A. M.; Rispens, M. T.; van Duren, J. K. J.; Hummelen, J. C.; Janssen, R. A. J. *J. Am. Chem. Soc.* **2001**, *123* (27), 6714−6715.

(85) Yang, C.; Li, H.; Sun, Q.; Qiao, J.; Li, Y.; Li, Y.; Zhu, D. *Sol. Energy Mater. Sol. Cells* **2005**, *85* (2), 241−249.

(86) Tan, Z. a.; Hou, J.; He, Y.; Zhou, E.; Yang, C.; Li, Y. *Macromolecules* **2007**, *40* (6), 1868−1873.

(87) Martín, N.; Sánchez, L.; Herranz, M. a. Á.; Illescas, B.; Guldi, D. M. *Acc. Chem. Res.* **2007**, *40* (10), 1015−1024.

(88) Hirayama, D.; Takimiya, K.; Aso, Y.; Otsubo, T.; Hasobe, T.; Yamada, H.; Imahori, H.; Fukuzumi, S.; Sakata, Y. *J. Am. Chem. Soc.* **2002**, *124* (4), 532−533.

(89) Miyanishi, S.; Zhang, Y.; Tajima, K.; Hashimoto, K. *Chem. Commun. (Cambridge, U. K.)* **2010**, *46* (36), 6723−6725.

(90) Cravino, A.; Sariciftci, N. S. *Nature Mater.* **2003**, *2* (6), 360−361.

(91) Roncali, J. *Adv. Energy Mater.* **2011**, *1* (2), 147−160.

(92) Svensson, M.; Zhang, F.; Veenstra, S. C.; Verhees, W. J. H.; Hummelen, J. C.; Kroon, J. M.; Inganäs, O.; Andersson, M. R. *Adv. Mater.* **2003**, *15* (12), 988−991.

(93) Peet, J.; Kim, J. Y.; Coates, N. E.; Ma, W. L.; Moses, D.; Heeger, A. J.; Bazan, G. C. *Nature Mater.* **2007**, *6* (7), 497−500.

(94) Price, S. C.; Stuart, A. C.; You, W. *Macromolecules* **2010**, *43* (2), 797−804.

(95) Svensson, M. *Synth. Met.* **2003**, *135−136*, 137−138.

(96) Hsu, S. L.-C.; Lin, Y.-C.; Lee, R.-F.; Sivakumar, C.; Chen, J.-S.; Chou, W.-Y. *J. Polym. Sci., Part A: Polym. Chem.* **2009**, *47* (20), 5336−5343.

(97) Kreyenschmidt, M.; Klaerner, G.; Fuhrer, T.; Ashenhurst, J.; Karg, S.; Chen, W. D.; Lee, V. Y.; Scott, J. C.; Miller, R. D. *Macromolecules* **1998**, *31* (4), 1099−1103.

(98) Yohannes, T.; Zhang, F.; Svensson, M.; Hummelen, J. C.; Andersson, M. R.; Inganäs, O. *Thin Solid Films* **2004**, *449* (1−2), 152−157.

(99) InganÄs, O.; Zhang, F.; Andersson, M. R. *Acc. Chem. Res.* **2009**, *42* (11), 1731−1739.

(100) Yang, R.; Tian, R.; Yan, J.; Zhang, Y.; Yang, J.; Hou, Q.; Yang, W.; Zhang, C.; Cao, Y. *Macromolecules* **2005**, *38* (2), 244−253.

(101) Janietz, S.; Krueger, H.; Schleiermacher, H.-F.; Würfel, U.; Niggemann, M. *Macromol. Chem. Phys.* **2009**, *210* (18), 1493−1503.

(102) Li, W.; Qin, R.; Zhou, Y.; Andersson, M.; Li, F.; Zhang, C.; Li, B.; Liu, Z.; Bo, Z.; Zhang, F. *Polymer* **2010**, *51* (14), 3031−3038.

(103) Zhou, E.; Cong, J.; Yamakawa, S.; Wei, Q.; Nakamura, M.; Tajima, K.; Yang, C.; Hashimoto, K. *Macromolecules* **2010**, *43* (6), 2873−2879.

(104) Mühlbacher, D.; Scharber, M.; Morana, M.; Zhu, Z.; Waller, D.; Gaudiana, R.; Brabec, C. *Adv. Mater.* **2006**, *18* (21), 2884−2889.

(105) Moulé, A. J.; Tsami, A.; Bünnagel, T. W.; Forster, M.; Kronenberg, N. M.; Scharber, M.; Koppe, M.; Morana, M.; Brabec, C. J.; Meerholz, K.; Scherf, U. *Chem. Mater.* **2008**, *20* (12), 4045−4050.

(106) Bijleveld, J. C.; Shahid, M.; Gilot, J.; Wienk, M. M.; Janssen, R. A. J. *Adv. Funct. Mater.* **2009**, *19* (20), 3262−3270.

(107) Zhou, H.; Yang, L.; Price, S. C.; Knight, K. J.; You, W. *Angew. Chem., Int. Ed.* **2010**, *49* (43), 7992−7995.

(108) Kudla, C. J.; Dolfen, D.; Schottler, K. J.; Koenen, J.-M.; Breusov, D.; Allard, S.; Scherf, U. *Macromolecules* **2010**, *43* (18), 7864−7867.

(109) Wang, E.; Wang, L.; Lan, L.; Luo, C.; Zhuang, W.; Peng, J.; Cao, Y. *Appl. Phys. Lett.* **2008**, *92* (3), 033307−033310.

(110) Zhou, E.; Wei, Q.; Yamakawa, S.; Zhang, Y.; Tajima, K.; Yang, C.; Hashimoto, K. *Macromolecules* **2009**, *43* (2), 821−826.

(111) Allard, N.; Aïch, R. d. B.; Gendron, D.; Boudreault, P.-L. T.; Tessier, C.; Alem, S.; Tse, S.-C.; Tao, Y.; Leclerc, M. *Macromolecules* **2010**, *43* (5), 2328−2333.

(112) Scharber, M. C.; Koppe, M.; Gao, J.; Cordella, F.; Loi, M. A.; Denk, P.; Morana, M.; Egelhaaf, H.-J.; Forberich, K.; Dennler, G.; Gaudiana, R.; Waller, D.; Zhu, Z.; Shi, X.; Brabec, C. J. *Adv. Mater.* **2010**, *22* (3), 367−370.

(113) Morana, M.; Azimi, H.; Dennler, G.; Egelhaaf, H.-J.; Scharber, M.; Forberich, K.; Hauch, J.; Gaudiana, R.; Waller, D.; Zhu, Z.; Hingerl, K.; van Bavel, S. S.; Loos, J.; Brabec, C. J. *Adv. Funct. Mater.* **2010**, *20* (7), 1180−1188.

(114) Veldman, D.; ipek, O. z.; Meskers, S. C. J.; Sweelssen, J. r.; Koetse, M. M.; Veenstra, S. C.; Kroon, J. M.; Bavel, S. S. v.; Loos, J.; Janssen, R. A. J. *J. Am. Chem. Soc.* **2008**, *130* (24), 7721−7735.

(115) Boudreault, P.-L. T.; Michaud, A.; Leclerc, M. *Macromol. Rapid Commun.* **2007**, *28* (22), 2176−2179.

(116) Zhou, E.; Nakamura, M.; Nishizawa, T.; Zhang, Y.; Wei, Q.; Tajima, K.; Yang, C.; Hashimoto, K. *Macromolecules* **2008**, *41* (22), 8302−8305.

(117) Liu, J.; Zhang, R.; Sauvé, G. v.; Kowalewski, T.; McCullough, R. D. *J. Am. Chem. Soc.* **2008**, *130* (39), 13167−13176.

(118) Zhou, E.; Yamakawa, S.; Tajima, K.; Yang, C.; Hashimoto, K. *Chem. Mater.* **2009**, *21* (17), 4055−4061.

(119) Morin, J.-F.; Leclerc, M.; Adès, D.; Siove, A. *Macromol. Rapid Commun.* **2005**, *26* (10), 761−778.

(120) Drolet, N.; Morin, J. F.; Leclerc, N.; Wakim, S.; Tao, Y.; Leclerc, M. *Adv. Funct. Mater.* **2005**, *15* (10), 1671−1682.

(121) Blouin, N.; Leclerc, M. *Acc. Chem. Res.* **2008**, *41* (9), 1110−1119.

(122) Chen, C.-P.; Chan, S.-H.; Chao, T.-C.; Ting, C.; Ko, B.-T. *J. Am. Chem. Soc.* **2008**, *130* (38), 12828−12833.

(123) Roncali, J. *Macromol. Rapid Commun.* **2007**, *28* (17), 1761−1775.

(124) Brédas, J. L.; Calbert, J. P.; da Silva Filho, D. A.; Cornil, J. *Proc. Natl. Acad. Sci. U. S. A.* **2002**, *99* (9), 5804−5809.

(125) Ando, S.; Nishida, J.-i.; Tada, H.; Inoue, Y.; Tokito, S.; Yamashita, Y. *J. Am. Chem. Soc.* **2005**, *127* (15), 5336−5337.

(126) Baek, N. S.; Hau, S. K.; Yip, H.-L.; Acton, O.; Chen, K.-S.; Jen, A. K. Y. *Chem. Mater.* **2008**, *20* (18), 5734−5736.

(127) Wu, J.-S.; Cheng, Y.-J.; Dubosc, M.; Hsieh, C.-H.; Chang, C.-Y.; Hsu, C.-S. *Chem. Commun. (Cambridge, U. K.)* **2010**, *46* (19), 3259−3261.

(128) Song, S.; Jin, Y.; Kim, S. H.; Moon, J.; Kim, K.; Kim, J. Y.; Park, S. H.; Lee, K.; Suh, H. *Macromolecules* **2008**, *41* (20), 7296−7305.

(129) Chen, Y.-C.; Yu, C.-Y.; Fan, Y.-L.; Hung, L.-I.; Chen, C.-P.; Ting, C. *Chem. Commun. (Cambridge, U. K.)* **2010**, *46* (35), 6503−6505.

(130) Hale, G. D.; Oldenburg, S. J.; Halas, N. J. *Appl. Phys. Lett.* **1997**, *71* (11), 1483−1485.

(131) Cumpston, B. H.; Jensen, K. F. *Synth. Met.* **1995**, *73* (3), 195−199.

(132) Wang, J.-Y.; Hau, S. K.; Yip, H.-L.; Davies, J. A.; Chen, K.-S.; Zhang, Y.; Sun, Y.; Jen, A. K. Y. *Chem. Mater.* **2011**, *23* (3), 765−767.

(133) Chen, C. H.; Cheng, Y. J.; Dubosc, M.; Hsieh, C. H.; Chu, C. C.; Hsu, C. S. *Chem.—Asian J.* **2010**, *5* (12), 2483−92.

(134) Xia, Y.; Su, X.; He, Z.; Ren, X.; Wu, H.; Cao, Y.; Fan, D. *Macromol. Rapid Commun.* **2010**, *31* (14), 1287−1292.

(135) Lee, T. W.; Kang, N. S.; Yu, J. W.; Hoang, M. H.; Kim, K. H.; Jin, J.-I.; Choi, D. H. *J. Polym. Sci., Part A: Polym. Chem.* **2010**, *48* (24), 5921−5929.

(136) Zhou, E.; Yamakawa, S.; Zhang, Y.; Tajima, K.; Yang, C.; Hashimoto, K. *J. Mater. Chem.* **2009**, *19* (41), 7730−7737.

(137) Lu, J.; Liang, F.; Drolet, N.; Ding, J.; Tao, Y.; Movileanu, R. *Chem. Commun. (Cambridge, U. K.)* **2008**, *44* (42), 5315−5317.

(138) Yu, C.-Y.; Chen, C.-P.; Chan, S.-H.; Hwang, G.-W.; Ting, C. *Chem. Mater.* **2009**, *21* (14), 3262−3269.

(139) Xiao, S.; Stuart, A. C.; Liu, S.; Zhou, H.; You, W. *Adv. Funct. Mater.* **2010**, *20* (4), 635−643.

(140) Coropceanu, V.; Kwon, O.; Wex, B.; Kaafarani, B. R.; Gruhn, N. E.; Durivage, J. C.; Neckers, D. C.; Brédas, J.-L. *Chem.—Eur. J.* **2006**, *12* (7), 2073−2080.

(141) Xiao, S.; Zhou, H.; You, W. *Macromolecules* **2008**, *41* (15), 5688−5696.

(142) Osaka, I.; Abe, T.; Shinamura, S.; Miyazaki, E.; Takimiya, K. *J. Am. Chem. Soc.* **2010**, *132* (14), 5000−5001.

(143) Laquindanum, J. G.; Katz, H. E.; Lovinger, A. J. *J. Am. Chem. Soc.* **1998**, *120* (4), 664−672.

(144) Jiang, Y.; Okamoto, T.; Becerril, H. A.; Hong, S.; Tang, M. L.; Mayer, A. C.; Parmer, J. E.; McGehee, M. D.; Bao, Z. *Macromolecules* **2010**, *43* (15), 6361−6367.

(145) Umeda, R.; Fukuda, H.; Miki, K.; Rahman, S. M. A.; Sonoda, M.; Tobe, Y. *C. R. Chim.* **2009**, *12* (3−4), 378−384.

(146) Loser, S.; Bruns, C. J.; Miyauchi, H.; Ortiz, R. o. P.; Facchetti, A.; Stupp, S. I.; Marks, T. J. *J. Am. Chem. Soc.* **2011**, *133* (21), 8142−8145.

(147) Mayer, A. C.; Toney, M. F.; Scully, S. R.; Rivnay, J.; Brabec, C. J.; Scharber, M.; Koppe, M.; Heeney, M.; McCulloch, I.; McGehee, M. D. *Adv. Funct. Mater.* **2009**, *19* (8), 1173−1179.

(148) Cates, N. C.; Gysel, R.; Dahl, J. E. P.; Sellinger, A.; McGehee, M. D. *Chem. Mater.* **2010**, *22* (11), 3543−3548.

(149) Xiao, S.; Stuart, A. C.; Liu, S.; You, W. *ACS Appl. Mater. Interfaces* **2009**, *1* (7), 1613−1621.

(150) Osaka, I.; Abe, T.; Shinamura, S.; Takimiya, K. *J. Am. Chem. Soc.* **2011**, *133* (17), 6852−6860.

(151) Shinamura, S.; Osaka, I.; Miyazaki, E.; Nakao, A.; Yamagishi, M.; Takeya, J.; Takimiya, K. *J. Am. Chem. Soc.* **2011**, *133* (13), 5024−5035.

(152) Rieger, R.; Beckmann, D.; Pisula, W.; Steffen, W.; Kastler, M.; Müllen, K. *Adv. Mater.* **2010**, *22* (1), 83−86.

(153) Rieger, R.; Beckmann, D.; Mavrinskiy, A.; Kastler, M.; Müllen, K. *Chem. Mater.* **2010**, *22* (18), 5314−5318.

(154) Hou, J.; Chen, H.-Y.; Zhang, S.; Li, G.; Yang, Y. *J. Am. Chem. Soc.* **2008**, *130* (48), 16144−16145.

(155) Blouin, N.; Michaud, A.; Leclerc, M. *Adv. Mater.* **2007**, *19* (17), 2295−2300.

(156) Blouin, N.; Michaud, A.; Gendron, D.; Wakim, S.; Blair, E.; Neagu-Plesu, R.; Belletete, M.; Durocher, G.; Tao, Y.; Leclerc, M. *J. Am. Chem. Soc.* **2008**, *130* (2), 732−742.

(157) Slooff, L. H.; Veenstra, S. C.; Kroon, J. M.; Moet, D. J. D.; Sweelssen, J.; Koetse, M. M. *Appl. Phys. Lett.* **2007**, *90* (14), 143506.

(158) Kline, R. J.; McGehee, M. D.; Kadnikova, E. N.; Liu, J.; Fréchet, J. M. J.; Toney, M. F. *Macromolecules* **2005**, *38* (8), 3312−3319.

(159) Zhou, H.; Yang, L.; Xiao, S.; Liu, S.; You, W. *Macromolecules* **2010**, *43* (2), 811−820.

(160) Wang, X.; Perzon, E.; Mammo, W.; Oswald, F.; Admassie, S.; Persson, N.-K.; Langa, F.; Andersson, M. R.; Inganaes, O. *Thin Solid Films* **2006**, *511−512* (1), 576−580.

(161) Tsai, J.-H.; Chueh, C.-C.; Lai, M.-H.; Wang, C.-F.; Chen, W.-C.; Ko, B.-T.; Ting, C. *Macromolecules* **2009**, *42* (6), 1897−1905.

(162) Lee, J.-Y.; Shin, W.-S.; Haw, J.-R.; Moon, D.-K. *J. Mater. Chem.* **2009**, *19* (28), 4938−4945.

(163) Padhy, H.; Huang, J.-H.; Sahu, D.; Patra, D.; Kekuda, D.; Chu, C.-W.; Lin, H.-C. *J. Polym. Sci., Part A: Polym. Chem.* **2010**, *48* (21), 4823−4834.

(164) Yang, R.; Tian, R.; Hou, Q.; Yang, W.; Cao, Y. *Macromolecules* **2003**, *36* (20), 7453−7460.

(165) Hou, J.; Chen, T. L.; Zhang, S.; Yang, Y. *J. Phys. Chem. C* **2009**, *113* (4), 1601−1605.

(166) Jung, I. H.; Kim, H.; Park, M.-J.; Kim, B.; Park, J.-H.; Jeong, E.; Woo, H. Y.; Yoo, S.; Shim, H.-K. *J. Polym. Sci., Part A: Polym. Chem.* **2010**, *48* (6), 1423−1432.

(167) Li, Z.; Ding, J.; Song, N.; Lu, J.; Tao, Y. *J. Am. Chem. Soc.* **2010**, *132* (38), 13160−13161.

(168) Wang, E.; Ma, Z.; Zhang, Z.; Henriksson, P.; Inganas, O.; Zhang, F.; Andersson, M. R. *Chem. Commun. (Cambridge, U. K.)* **2011**, *47* (17), 4908−4910.

(169) Bijleveld, J. C.; Gevaerts, V. S.; Di, N. D.; Turbiez, M.; Mathijssen, S. G. J.; de, L. D. M.; Wienk, M. M.; Janssen, R. A. J. *Adv. Mater.* **2010**, *22* (35), E242−E246.

(170) Liu, B.; Zou, Y.; Peng, B.; Zhao, B.; Huang, K.; He, Y.; Pan, C. *Polym. Chem.* **2011**, *2* (5), 1156−1162.

(171) Mei, J.; Graham, K. R.; Stalder, R.; Reynolds, J. R. *Org. Lett.* **2010**, *12* (4), 660−663.

(172) Wienk, M. M.; Turbiez, M.; Gilot, J.; Janssen, R. A. J. *Adv. Mater.* **2008**, *20* (13), 2556−2560.

(173) Zou, Y.; Gendron, D.; Badrou-Aïch, R. d.; Najari, A.; Tao, Y.; Leclerc, M. *Macromolecules* **2009**, *42* (8), 2891−2894.

(174) Huo, L.; Hou, J.; Chen, H.-Y.; Zhang, S.; Jiang, Y.; Chen, T. L.; Yang, Y. *Macromolecules* **2009**, *42* (17), 6564−6571.

(175) Woo, C. H.; Beaujuge, P. M.; Holcombe, T. W.; Lee, O. P.; Frechet, J. M. J. *J. Am. Chem. Soc.* **2010**, *132* (44), 15547−15549.

(176) Bronstein, H.; Chen, Z.; Ashraf, R. S.; Zhang, W.; Du, J.; Durrant, J. R.; Shakya, T. P.; Song, K.; Watkins, S. E.; Geerts, Y.; Wienk, M. M.; Janssen, R. A. J.; Anthopoulos, T.; Sirringhaus, H.; Heeney, M.; McCulloch, I. *J. Am. Chem. Soc.* **2011**, *133* (10), 3272−3275.

(177) Zou, Y.; Najari, A.; Berrouard, P.; Beaupre, S.; Reda, A. B.; Tao, Y.; Leclerc, M. *J. Am. Chem. Soc.* **2010**, *132* (15), 5330−5331.

(178) Zhang, Y.; Hau, S. K.; Yip, H.-L.; Sun, Y.; Acton, O.; Jen, A. K. Y. *Chem. Mater.* **2010**, *22* (9), 2696−2698.

(179) Zhang, G.; Fu, Y.; Zhang, Q.; Xie, Z. *Chem. Commun. (Cambridge, U. K.)* **2010**, *46* (27), 4997−4999.

(180) Piliego, C.; Holcombe, T. W.; Douglas, J. D.; Woo, C. H.; Beaujuge, P. M.; Frechet, J. M. J. *J. Am. Chem. Soc.* **2010**, *132* (22), 7595−7597.

(181) Li, Z.; Tsang, S.-W.; Du, X.; Scoles, L.; Robertson, G.; Zhang, Y.; Toll, F.; Tao, Y.; Lu, J.; Ding, J. *Adv. Funct. Mater.* **2011**, *21* (17), 3331−3336.

(182) Bundgaard, E.; Krebs, F. C. *Macromolecules* **2006**, *39* (8), 2823−2831.

(183) Perzon, E.; Wang, X.; Zhang, F.; Mammo, W.; Delgado, J. L.; de la Cruz, P.; Inganäs, O.; Langa, F.; Andersson, M. R. *Synth. Met.* **2005**, *154* (1−3), 53−56.

(184) Wang, X.; Perzon, E.; Delgado, J. L.; de la Cruz, P.; Zhang, F.; Langa, F.; Andersson, M.; Inganas, O. *Appl. Phys. Lett.* **2004**, *85* (21), 5081−5083.

(185) Zhang, F.; Bijleveld, J.; Perzon, E.; Tvingstedt, K.; Barrau, S.; Inganas, O.; Andersson, M. R. *J. Mater. Chem.* **2008**, *18* (45), 5468−5474.

(186) Gendron, D.; Morin, P.-O.; Najari, A.; Leclerc, M. *Macromol. Rapid Commun.* **2010**, *31* (12), 1090−1094.

(187) Brédas, J. L.; Heeger, A. J. *Chem. Phys. Lett.* **1994**, *217* (5−6), 507−512.

(188) Helbig, M.; Hörhold, H.-H. *Makromol. Chem.* **1993**, *194* (6), 1607−1618.

(189) Greenham, N. C.; Moratti, S. C.; Bradley, D. D. C.; Friend, R. H.; Holmes, A. B. *Nature (London, U. K.)* **1993**, *365* (6447), 628−630.

(190) Wong, S.; Ma, H.; Jen, A. K. Y.; Barto, R.; Frank, C. W. *Macromolecules* **2003**, *36* (21), 8001−8007.

(191) Reichenbacher, K.; Suss, H. I.; Hulliger, J. *Chem. Soc. Rev.* **2005**, *34* (1), 22−30.

(192) Pagliaro, M.; Ciriminna, R. *J. Mater. Chem.* **2005**, *15* (47), 4981−4991.

(193) Wang, Y.; Parkin, S. R.; Gierschner, J.; Watson, M. D. *Org. Lett.* **2008**, *10* (15), 3307−3310.

(194) Liang, Y.; Feng, D.; Wu, Y.; Tsai, S.-T.; Li, G.; Ray, C.; Yu, L. *J. Am. Chem. Soc.* **2009**, *131* (22), 7792−7799.

(195) Liang, Y.; Yu, L. *Acc. Chem. Res.* **2010**, *43* (9), 1227−1236.

(196) Cho, S.; Seo, J. H.; Kim, S. H.; Song, S.; Jin, Y.; Lee, K.; Suh, H.; Heeger, A. J. *Appl. Phys. Lett.* **2008**, *93* (26), 263301−263303.

(197) Jayakannan, M.; Van Hal, P. A.; Janssen, R. A. J. *J. Polym. Sci., Part A: Polym. Chem.* **2002**, *40* (2), 251−261.

(198) Karikomi, M.; Kitamura, C.; Tanaka, S.; Yamashita, Y. *J. Am. Chem. Soc.* **2002**, *117* (25), 6791−6792.

(199) Wang, E.; Wang, M.; Wang, L.; Duan, C.; Zhang, J.; Cai, W.; He, C.; Wu, H.; Cao, Y. *Macromolecules* **2009**, *42* (13), 4410−4415.

(200) Gadisa, A.; Oosterbaan, W. D.; Vandewal, K.; Bolsée, J.-C.; Bertho, S.; D'Haen, J.; Lutsen, L.; Vanderzande, D.; Manca, J. V. *Adv. Funct. Mater.* **2009**, *19* (20), 3300−3306.

(201) Egbe, D. A. M.; Türk, S.; Rathgeber, S.; Kühnlenz, F.; Jadhav, R.; Wild, A.; Birckner, E.; Adam, G.; Pivrikas, A.; Cimrova, V.; Knör, G. n.; Sariciftci, N. S.; Hoppe, H. *Macromolecules* **2010**, *43* (3), 1261−1269.

(202) Szarko, J. M.; Guo, J.; Liang, Y.; Lee, B.; Rolczynski, B. S.; Strzalka, J.; Xu, T.; Loser, S.; Marks, T. J.; Yu, L.; Chen, L. X. *Adv. Mater.* **2010**, *22* (48), 5468−5472.

(203) Shi, C. J.; Yao, Y.; Yang, Y.; Pei, Q. B. *J. Am. Chem. Soc.* **2006**, *128* (27), 8980−8986.

(204) Hou, J.; Chen, H.-Y.; Zhang, S.; Yang, Y. *J. Phys. Chem. C* **2009**, *113* (50), 21202−21207.

(205) Hou, J.; Chen, H.-Y.; Zhang, S.; Chen, R. I.; Yang, Y.; Wu, Y.; Li, G. *J. Am. Chem. Soc.* **2009**, *131* (43), 15586−15587.

(206) Price, S. C.; Stuart, A. C.; You, W. *Macromolecules* **2010**, *43* (10), 4609−4612.

(207) Bagnis, D.; Beverina, L.; Huang, H.; Silvestri, F.; Yao, Y.; Yan, H.; Pagani, G. A.; Marks, T. J.; Facchetti, A. *J. Am. Chem. Soc.* **2010**, *132* (12), 4074−4075.

(208) Clarke, T. M.; Durrant, J. R. *Chem. Rev. (Washington, DC, U. S.)* **2010**, *110* (11), 6736−6767.

(209) Zhu, X. Y.; Yang, Q.; Muntwiler, M. *Acc. Chem. Res.* **2009**, *42* (11), 1779−1787.

(210) Deibel, C.; Dyakonov, V. *Rep. Prog. Phys.* **2010**, *73* (9), 096401.

(211) Peet, J.; Heeger, A. J.; Bazan, G. C. *Acc. Chem. Res.* **2009**, *42* (11), 1700−1708.

(212) Peet, J.; Senatore, M. L.; Heeger, A. J.; Bazan, G. C. *Adv. Mater.* **2009**, *21* (14−15), 1521−1527.

(213) Moulé, A. J.; Meerholz, K. *Adv. Funct. Mater.* **2009**, *19* (19), 3028−3036.

(214) van Bavel, S.; Veenstra, S.; Loos, J. *Macromol. Rapid Commun.* **2010**, *31* (21), 1835−1845.

(215) Groves, C.; Reid, O. G.; Ginger, D. S. *Acc. Chem. Res.* **2010**, *43* (5), 612−620.

(216) Chen, L.-M.; Hong, Z.; Li, G.; Yang, Y. *Adv. Mater.* **2009**, *21* (14−15), 1434−1449.

(217) Huo, L.; Zhang, S.; Guo, X.; Xu, F.; Li, Y.; Hou, J. *Angew. Chem., Int. Ed.* **2011**, *50* (41), 9697−9702.

(218) Kotlarski, J. D.; Blom, P. W. M. *Appl. Phys. Lett.* **2011**, *98* (5), 053301−053303.

(219) http://www.flisom.ch/.

(220) http://www.q-cells.com/en/index.html.

(221) Hou, J.; Tan, Z. a.; Yan, Y.; He, Y.; Yang, C.; Li, Y. *J. Am. Chem. Soc.* **2006**, *128* (14), 4911−4916.

(222) Zhou, E.; Cong, J.; Wei, Q.; Tajima, K.; Yang, C.; Hashimoto, K. *Angew. Chem., Int. Ed.* **2011**, *50* (12), 2799−2803.

(223) Schlenker, C. W.; Thompson, M. E. *Chem. Commun. (Cambridge, U. K.)* **2011**, *47* (13), 3702−3716.

(224) Brunetti, F. G.; Gong, X.; Tong, M.; Heeger, A. J.; Wudl, F. *Angew. Chem., Int. Ed.* **2010**, *49* (3), 532−536.

(225) Gong, X.; Tong, M.; Brunetti, F. G.; Seo, J.; Sun, Y.; Moses, D.; Wudl, F.; Heeger, A. J. *Adv. Mater.* **2011**, *23* (20), 2272−2277.

(226) Street, R. A. *Appl. Phys. Lett.* **2008**, *93* (13), 133308−133311.

(227) Varotto, A.; Treat, N. D.; Jo, J.; Shuttle, C. G.; Batara, N. A.; Brunetti, F. G.; Seo, J. H.; Chabinyc, M. L.; Hawker, C. J.; Heeger, A. J.; Wudl, F. *Angew. Chem., Int. Ed.* **2011**, *50* (22), 5166−5169.

(228) Brabec, C. J.; Heeney, M.; McCulloch, I.; Nelson, J. *Chem. Soc. Rev.* **2011**, *40* (3), 1185−1199.

(229) Cates, N. C.; Gysel, R.; Beiley, Z.; Miller, C. E.; Toney, M. F.; Heeney, M.; McCulloch, I.; McGehee, M. D. *Nano Lett.* **2009**, *9* (12), 4153−4157.

(230) Steim, R.; Kogler, F. R.; Brabec, C. J. *J. Mater. Chem.* **2010**, *20* (13), 2499−2512.

(231) Chen, L.-M.; Xu, Z.; Hong, Z.; Yang, Y. *J. Mater. Chem.* **2010**, *20* (13), 2575−2598.

(232) Irwin, M. D.; Buchholz, D. B.; Hains, A. W.; Chang, R. P. H; Marks, T. J. *Proc. Natl. Acad. Sci. U. S. A.* **2008**, *105* (8), 2783−2787.

(233) Sun, Y.; Takacs, C. J.; Cowan, S. R.; Seo, J. H.; Gong, X.; Roy, A.; Heeger, A. J. *Adv. Mater.* **2011**, *23* (19), 2226−2230.

(234) Subbiah, J.; Kim, D. Y.; Hartel, M.; So, F. *Appl. Phys. Lett.* **2010**, *96* (6), 063303−063306.

(235) Kröger, M.; Hamwi, S.; Meyer, J.; Riedl, T.; Kowalsky, W.; Kahn, A. *Appl. Phys. Lett.* **2009**, *95* (12), 123301−123304.

(236) Tao, C.; Ruan, S. P.; Xie, G. H.; Kong, X. Z.; Shen, L.; Meng, F. X.; Liu, C. X.; Zhang, X. D.; Dong, W.; Chen, W. Y. *Appl. Phys. Lett.* **2009**, *94* (4), 043311−043314.

(237) Meyer, J.; Kroger, M.; Hamwi, S.; Gnam, F.; Riedl, T.; Kowalsky, W.; Kahn, A. *Appl. Phys. Lett.* **2010**, *96* (19), 193302−193305.

(238) Hayakawa, A.; Yoshikawa, O.; Fujieda, T.; Uehara, K.; Yoshikawaa, S. *Appl. Phys. Lett.* **2007**, *90* (16), 163517−163520.

(239) Sun, Y.; Seo, J. H.; Takacs, C. J.; Seifter, J.; Heeger, A. J. *Adv. Mater.* **2011**, *23* (14), 1679−1683.

(240) Yip, H.-L.; Hau, S. K.; Baek, N. S.; Ma, H.; Jen, A. K. Y. *Adv. Mater.* **2008**, *20* (12), 2376−2382.

(241) Bulliard, X.; Ihn, S.-G.; Yun, S.; Kim, Y.; Choi, D.; Choi, J.-Y.; Kim, M.; Sim, M.; Park, J.-H.; Choi, W.; Cho, K. *Adv. Funct. Mater.* **2010**, *20* (24), 4381−4387.

(242) Chang, C.-Y.; Wu, C.-E.; Chen, S.-Y.; Cui, C.; Cheng, Y.-J.; Hsu, C.-S.; Wang, Y.-L.; Li, Y. *Angew. Chem., Int. Ed.* **2011**, *50* (40), 9386−9390.

(243) Ameri, T.; Dennler, G.; Waldauf, C.; Azimi, H.; Seemann, A.; Forberich, K.; Hauch, J.; Scharber, M.; Hingerl, K.; Brabec, C. J. *Adv. Funct. Mater.* **2010**, *20* (10), 1592−1598.

(244) Ko, D.-H.; Tumbleston, J. R.; Zhang, L.; Williams, S.; DeSimone, J. M.; Lopez, R.; Samulski, E. T. *Nano Lett.* **2009**, *9* (7), 2742−2746.

(245) Hadipour, A.; de Boer, B.; Blom, P. W. M. *Adv. Funct. Mater.* **2008**, *18* (2), 169−181.

(246) Hu, L.; Hecht, D. S.; Grüner, G. *Nano Lett.* **2004**, *4* (12), 2513−2517.

(247) Wu, Z.; Chen, Z.; Du, X.; Logan, J. M.; Sippel, J.; Nikolou, M.; Kamaras, K.; Reynolds, J. R.; Tanner, D. B.; Hebard, A. F.; Rinzler, A. G. *Science (Washington, DC, U. S.)* **2004**, *305* (5688), 1273−1276.

(248) Zhang, M.; Fang, S.; Zakhidov, A. A.; Lee, S. B.; Aliev, A. E.; Williams, C. D.; Atkinson, K. R.; Baughman, R. H. *Science (Washington, DC, U. S.)* **2005**, *309* (5738), 1215−1219.

(249) Li, J.; Hu, L.; Wang, L.; Zhou, Y.; Grüner, G.; Marks, T. J. *Nano Lett.* **2006**, *6* (11), 2472−2477.

(250) Miller, A. J.; Hatton, R. A.; Silva, S. R. P. *Appl. Phys. Lett.* **2006**, *89* (13), 133117−133120.

(251) Rowell, M. W.; Topinka, M. A.; McGehee, M. D.; Prall, H.-J.; Dennler, G.; Sariciftci, N. S.; Hu, L.; Gruner, G. *Appl. Phys. Lett.* **2006**, *88* (23), 233506−233509.

(252) Eda, G.; Fanchini, G.; Chhowalla, M. *Nature Nanotechnol.* **2008**, *3* (5), 270−274.

(253) Kim, K. S.; Zhao, Y.; Jang, H.; Lee, S. Y.; Kim, J. M.; Kim, K. S.; Ahn, J.-H.; Kim, P.; Choi, J.-Y.; Hong, B. H. *Nature (London, U. K.)* **2009**, *457* (7230), 706−710.

(254) Gomez De Arco, L.; Zhang, Y.; Schlenker, C. W.; Ryu, K.; Thompson, M. E.; Zhou, C. *ACS Nano* **2010**, *4* (5), 2865−2873.

(255) Gaynor, W.; Burkhard, G. F.; McGehee, M. D.; Peumans, P. *Adv. Mater.* **2011**, *23* (26), 2905−2910.

(256) Yang, L.; Zhang, T.; Zhou, H.; Price, S. C.; Wiley, B. J.; You, W. *ACS Appl. Mater. Interfaces* **2011**, *3* (10), 4075−4084.

(257) http://www.konarka.com/.